Title: Megakaryopoiesis in Dengue virus infected K562 cell promotes viral replication which inhibits endomitosis and accumulation of ROS associated with differentiation

Jaskaran Kaur *[1], Yogita Rawat *[1], Vikas Sood[2], Deepak K. Rathore[1], Shrikant K. Kumar[1], Niraj K. Kumar[1] and Sankar Bhattacharyya[1]

[1] *Translational Health Science and Technology Institute, NCR Biotech Science Cluster, PO Box# 4, Faridabad-Gurgaon expressway, Faridabad, Haryana-121001, India*

[2] *Department of Biochemistry, School of Chemical and Life Sciences, Jamia Hamdard (Hamdard University) Hamdard Nagar, New Delhi - 110062, India*

*Equal contribution

Email for correspondence: sankar@thsti.res.in

Keywords: Dengue virus replication, Megakaryopoiesis, Reactive oxygen species, Endomitosis

Abstract: In the human host blood Monocytes and bone marrow Megakaryocytes are implicated as major sites supporting high replication. The human K562 cell line supports DENV replication and represent Megakaryocyte-Erythrocyte progenitors (MEP), replicating features of *in vivo* Megakaryopoiesis upon stimulation with Phorbol esters. In this article, we report results that indicate the mutual influence of Megakaryopoiesis and DENV replication on each other, through comparison of PMA-induced differentiation of either mock-infected or DENV-infected K562 cells. We present data showing PMA-induced differentiation to drastically increase DENV replication and a concomitant augmented secretion of infectious virus. Although the mechanism is not clear yet, we show that it is not through an increased uptake of virus by differentiated cells. On the other hand, DENV replication in cells undergoing PMA-induced differentiation, interferes with major differentiation markers of Megakaryopoiesis including activation of ERK1/2 MAP Kinase, endomitosis and surface expression of platelet-specific proteins without any drastic effect on cell death. Among signaling intermediaries of the JAK-STAT pathway, we observed infection associated degradation of SOC3 protein similar to earlier observations with STAT2. DENV infection leads to accumulation of Reactive-oxygen species (ROS) in different cells including K562. PMA-induced differentiation of uninfected K562 cells also leads to intracellular ROS accumulation. Interestingly, we observed ROS accumulation to be suppressed by concomitant DENV replication in K562 cells undergoing PMA-induced differentiation. This is the first report of a model system where DENV replication suppresses intracellular ROS accumulation. The implications of these results for Megakaryopoiesis and viral replication would be discussed.

36 **Introduction**

37 Platelets play a unique role in tissue homeostasis and regulation of inflammation. The abundance of these
38 small, anuclear cells produced from specialized cells called Megakaryocytes (MKs) in the bone marrow
39 (BM) is controlled by a steady rate of biogenesis (about $1x10^9$/day) and decay, with an average life of 7
40 days in humans (1). A perturbation of platelet homeostasis is associated with infection by multiple human
41 pathogenic viruses (2). Infection by Dengue virus (DENV) a member of the Flaviviridae, can cause an acute
42 febrile illness with the potential to turn fatal. Beside humans, DENV can infect mosquitoes and these
43 transmit infectious virus along with salivary fluid during a blood meal. Only about a quarter of infected
44 humans exhibit clinical symptoms that include high fever, retro-orbital pain, muscle pain,
45 thrombocytopenia or drop in platelet level etc. that subside after 4-7 days. Subsequently a proportion of
46 symptomatic individuals develop symptoms of severe Dengue characterized by leakage of fluid from the
47 blood vessels, leading to reduction in blood volume in addition to acute thrombocytopenia (3). Multiple
48 mechanisms working in parallel have been suggested to contribute to the thrombocytopenia associated with
49 Dengue infection which include inhibition of platelet biogenesis by infection of Megakaryocytes,
50 augmented platelet decay through either a direct interaction with the virus or upon binding of anti-platelet
51 antibodies (4).

52 Depending on the cell type the entry of DENV can be mediated by different surface receptors and
53 the complex is endocytosed into endosome following virus binding (5) Acidification of these endosomes
54 by their membrane resident proton pumps induce a fusion between the viral and endosomal membranes
55 leading to release of the viral genome into host cytosol. The genome of DENV is a ~11 kb long single-
56 stranded plus-sense RNA coding for one large polyprotein which is then cleaved to generate the structural
57 (Core or C, Envelop or E and precursor-Membrane or prM) and non-structural proteins (NS1, NS2A, NS2B,
58 NS3, NS4A, NS4B and NS5) of the virus. After few rounds of translation the viral genomic RNA undergoes
59 replication in **r**eplication **c**omplexes (RC) that are associated with the host cell **E**ndoplasmic **r**eticulum
60 (ER). The NS5 protein performs crucial function in replication of the genome by polymerizing both

61 negative and positive strand genomic RNA through asymmetric replication in favor of the later. Among
62 these only the plus-sense genomic RNA is capped by a Methyl-transferase (MTase) domain also harbored
63 in the NS5, followed by encapsidation of the genomic RNA by the Core or C protein. The newly assembled
64 virus particles contain a RNA-protein complex consisting of a single copy of the genomic RNA with
65 multiple copies of the C protein, encased in a membrane studded with E and prM protein. These transit
66 through the protein secretory pathway of the host cell where the prM protein is cleaved by a host protease
67 called Furin to produce M protein. The virion particles containing M protein along with E in the envelope
68 are released from the host cell without lysis (6).

69 DENV can infect multiple cell types in the human body including monocytes in the blood,
70 megakaryocytes in the BM and hepatocytes in the liver (5, 7). In addition to these DENV can activate
71 platelets, through a direct interaction with viral receptors on the cell surface (5, 8, 9). Platelets activated by
72 DENV secrete a number of cytokines and chemokines among which CXCL4 promotes viral replication in
73 infected Monocytes, upon binding to CXCR3 receptors on these cells (10). Myelosuppression or a reduction
74 in the mass of BM cells is one of the hallmarks of DENV infection and cells of Megakaryocytic cells have
75 been shown to be particularly permissive to viral replication (11-14). This suggested MK cells to
76 significantly contribute to viremia beside monocytes. In addition the survival of megakaryocytes have been
77 suggested to be negatively affected by infection, thereby leading to reduced platelet biogenesis which
78 contributes to DENV associated thrombocytopenia (15).

79 Hematopoietic stem cells (HSC) in the BM differentiate into multiple lineages producing all cell
80 types in the blood. One of such lineages are composed of bi-potential Megakaryocyte-Erythrocyte
81 progenitor (MEP) cells that can differentiate into either cell type (16, 17). Differentiation of MEP into a
82 MK involves profound cellular and molecular changes including cell expansion, endomitosis which
83 generates a multi-lobed and polyploid nucleus and expression of platelet specific surface markers on the
84 plasma membrane which will become part of the platelets membrane (18, 19). Platelets bud off from the
85 MK along with a bit of its cytoplasm, containing granules of different types and a host of specific mRNAs

86 (20). Differentiation of MEPs into MKs is promoted by a number of cytokines, the most characterized
87 among which is Thrombopoietin or TPO that binds to the TPO-receptor c-Mpl on the cell surface (21).
88 TPO binding to c-Mpl activates Janus Kinase 2 (JAK2) receptor tyrosine kinase which in turn transduces
89 the signal through specific **S**ignal **t**ransducer and **a**ctivator of **t**ranscription or STATs (STA3 and STAT5),
90 **M**itogen-**a**ctivated **p**rotein **k**inases or MAPK (ERK1/2) and the Phosphatidyl Inosine-3 or PI-3 Kinase (22).
91 STAT3 and STAT5 have been shown to have opposing function in Megakaryopoiesis with the former
92 promoting it (23, 24). Activation of JAK2 pathway increases expression of pro-inflammatory genes and in
93 fact activating these genes through exogenous activation of Toll-like receptor 2 or TLR2 has been shown
94 to promote megakaryocyte development (25). In a similar manner, the activation of ERK1/2 MAPK and
95 inhibition of p38-MAPK promotes Megakaryopoiesis by playing a crucial role in endomitosis (26).
96 Transduction of the signal from JAK2 leads to activated transcription by a number of transcription factors
97 (TFs) increasing the expression of specific genes (27, 28). TFs like GATA-1 and RUNX1 play crucial role
98 in endomitosis through upregulation of CyclinD1 (29, 30). In addition to these different specific pathways
99 like ER-stress and Autophagy have been shown to play role in Megakaryopoiesis (31). A controlled form
100 of apoptosis is known to be crucial for production of platelets from megakaryocytes and ER-stress has been
101 suggested to play a role in this apoptosis (31-33). In the BM, HSCs occupy a relatively hypoxic niche
102 compared to more differentiated lineages, particularly the MKs which shed mature platelets into the blood
103 vasculature. This migration from hypoxic to normoxic environment increases the level of reactive oxygen
104 species (ROS) in these cells, which has been indicated as a crucial signaling molecules (34). In fact
105 increased oxygen level and augmented expression of ROS generating enzymes show positive correlation
106 with megakaryocyte development, corroborating ROS to serve a critical promoter of megakaryopoiesis (35-
107 37). ROS has been suggested to function at multiple levels which include increasing the level of tyrosine-
108 phosphorylation on some proteins or by inhibition certain tyrosine phosphatases or by maintenance of ERK
109 activation or modulation of cyclin levels or increasing expression of crucial TFs or promoting
110 differentiation associated apoptosis (35, 38-40).

111 K562 cells represent a bi-potential cell line which can be differentiated to either MK-like cells or
112 Erythroblast-like cells depending on differential pharmacological stimulation (41). Supplementation of
113 Phorbol esters like Phorbol-12 myristate-13 (PMA) in growth media of K562 cells drives differentiation
114 towards megakaryocytes, inducing cellular and molecular changes akin to MKs *in vivo,* through activation
115 of identical signaling axes (42-50). In addition to this K562 is permissible to DENV replication and is
116 therefore a good model system to study the effect of DENV infection on Megakaryopoiesis (51). In this
117 report we show results suggesting that when DENV infected MEPs differentiate into megakaryocytes the
118 intracellular viral replication is promoted, by a mechanism that is not clear yet. This enhancement of viral
119 replication affects key signaling pathways that are known to be crucial for maturation of megakaryocytes,
120 without any significant effect on their survival. DENV infection is known to induce an accumulation of
121 ROS in the host cells. K562 cells induced to differentiate into megakaryocytes by treatment with PMA also
122 accumulate ROS. However surprisingly, infected cells undergoing differentiation accumulate significantly
123 less ROS when compared to uninfected controls, suggesting an active suppression of ROS by viral
124 replication. The implications of these observations with respect to Megakaryopoiesis and DENV replication
125 have been discussed.

126

127 **Results:**

128 **K562 cells recapitulate major events in Megakaryopoiesis upon PMA-treatment**

129 Differentiation of Mk from an MEP follows elaborate cellular changes involving a dramatic increase in cell
130 size and endomitosis with consequential formation of a multi-lobed, polyploid nucleus as depicted in the
131 schematic figure (Fig. 1A.). K562 cells mimic a bi-potential Megakaryocyte-Erythrocyte progenitor (MEP)
132 and depending upon pharmacological treatment can be differentiated into cells of either Mk-lineage
133 (Phorbol esters) or Erythroblast-lineage (Sodium Butyrate or NaB) (41). Upon supplementation of Phorbol-
134 12 Myristate-13 acetate (PMA) in culture media, K562 cells stopped proliferation and enlarged in size (data
135 not shown). Further, the cells underwent endomitosis leading to generation of polyploid cells harboring
136 multilobed nuclei (Fig. 1B.). When analyzed by flow cytometry, the side scatter of PMA-treated K562 cells
137 showed a significant increase indicating accumulation of cytoplasmic granules (data not shown). The
138 platelet plasma membrane is derived from that of the Mk mother cell and during differentiation platelet-
139 specific surface markers are expressed on the Mk surface. As a corroboration of megakaryopoiesis induced
140 by PMA-treatment, the surface expression of three platelet specific markers were quantified in K562 cells
141 and the result showed a dramatic increase in the level of CD41/61, CD61 alone and a significant increase
142 in number of cells positive for CD42b expression (Fig. 1C.). Analysis of the cell ploidy following PMA-
143 treatment showed an almost complete disappearance of cells in the S-phase and emergence of polyploid
144 cells with ploidy of 8N and 16N (Fig. 1D.). As a control for these changes being specific to K562, PMA-
145 supplementation did not stall the growth or induce expression of platelet-specific surface markers in cells
146 of the hepatoma cell line Huh7 (data not shown). Since treatment with NaB induces differentiation towards
147 an Erythroblast-lineage, the differential expression of specific genes were compared between K562 cells
148 treated with either PMA or NaB. The result showed a distinct pattern of gene expression induced by these
149 pharmacological treatments differentiating the two lineages, especially with respect to transcripts of the
150 gene GATA2, EBP42, GYPA and CD61 (Fig. 1E.).

151

152

153 **Differentiation of K562-MKs promote replication of Dengue virus**

154 Differentiation into megakaryocytes is associated with arrest in cell cycle and other molecular changes. In
155 order to analyze how these changes might affect the ongoing intracellular replication process, DENV
156 replication in infected K562 cells that have been treated with PMA soon after infection, was compared to
157 simultaneously infected cells treated with vehicle (DMSO). For this purpose, the level of DENV envelope
158 protein accumulated was compared between these conditions at 3 or 6 days post-infection by
159 immunofluorescence followed by analysis in a flow cytometer. The result showed that although the viral
160 protein accumulated at 3 days p.i was comparable between PMA-treated and DMSO-treated cells, a
161 dramatic difference between them was observed at day 6 (Fig. 2A.). This difference was observed using
162 different MOI of infection, although due to saturation of immunostaining the difference was less dramatic
163 at higher MOI (data not shown). In order to check if higher accumulation of viral protein correlates
164 positively with viral replication, the level of intracellular viral RNA and infectious virus in culture
165 supernatant was compared between infected K562 cells treated with either PMA or DMSO for 3 or 6 days.
166 The results showed a similar higher accumulation of intracellular viral genomic RNA and extracellular
167 infectious virus, between these two conditions at 6 days post-infection (Fig. 2B and 2C). During virus
168 maturation the prM protein on assembled virion particles undergoes a cleavage by the host protease Furin,
169 a step necessary for conferring infectivity to the secreted virus (52). Therefore the comparatively higher
170 infectious titer in culture supernatant of PMA-treated cells can result from either higher secretion of virus
171 (more virion particles without any change in their infectivity) or more efficient Furin cleavage brought
172 about by the cellular and biochemical changes accompanying differentiation (same number of virion
173 particles as secreted by DMSO-treated cells but with higher infectivity). To dissect these possibilities, the
174 viral genomic RNA from culture supernatant of cells kept with either PMA or DMSO was extracted and
175 purified and their relative level compared by real-time PCR using DENV specific oligonucleotide primers.
176 The comparison showed comparatively more viral genomic RNA in the supernatant of PMA-treated cells,

177 suggesting that the differentiating cells secrete more virus that are produced by higher replication efficiency
178 in these cells (data not shown). However this indicated towards possibilities wherein the entry within
179 differentiating cells might be facilitated e.g. through overexpression of viral receptor. In order to address
180 this, uninfected K562 cells treated with either DMSO or PMA for 3 days were incubated with DENV
181 inoculum and the viral entry compared by comparison of the internalized genomic RNA immediately after
182 entry. The result showed a comparable entry into cells irrespective of no differentiation or differentiation
183 for 3 days, implying that the promotion of replication occurs post-entry (Fig. 2D). As a negative control
184 DENV-infected Huh7 cells did not exhibit any differential replication depending on treatment with PMA
185 and DMSO (data not shown). Also, treatment of infected K562 cells with Na-butyrate which would initiate
186 erythropoiesis, did not exhibit a similar promotion of the viral replication (data not shown).

187 **Cellular and biochemical changes imposed by DENV infection in differentiating K562 cells**

188 Differentiation of Mk from HSCs is influenced by multiple cytokines, the most characterized among which
189 is Thrombopoietin (TPO) which is secreted from liver cells and binds to the surface receptor c-Mpl.
190 Interaction of TPO with c-MPL activates Janus kinase 2 (JAK2) tyrosine kinase initiating a cascade of
191 phosphorylation events (Fig. 3A). Although an important cytokine, TPO is not indispensable for
192 megakaryopoiesis since a knock-out of the gene encoding TPO ($TPO^{-/-}$) is not lethal in mice, albeit with the
193 platelet level being at 10% of that in wild-type animals. Phorbol esters like PMA are known to activate
194 kinases like Protein kinase-C (PKC) that in its turn transduces the signal through nodes many of which are
195 shared with TPO signaling. In response to viral infection mammalian cells secrete cytokines like Interferons
196 that bind to cell surface receptors either in an autocrine or paracrine manner and induce an 'anti-viral' state
197 within the cell. JAK2 is also central to signaling via the interferon receptor consequent to binding of type-
198 I IFNs to the receptor (IFNR). This implied that megakaryopoiesis even when it is PMA-induced would
199 potentially create an antiviral state within the cell and in that context it would be interesting to observe how
200 DENV is still able to replicate to higher extent compared to undifferentiated cells. Since both of these
201 pathways would also be potentially perturbed by a virus infection, we investigated the status of different

202 members by immunoblotting, in cells which were stimulated to undergo PMA-dependent differentiation
203 immediately after infection.

204 Phosphorylation of the MAPK ERK1/2 plays a crucial role in MK development and expectedly we observed
205 an increase in the ratio of p-ERK/ERK both subsequent time points when compared to day 0 (Fig. 3B,
206 compare lanes 2 and 5 with lane 1**)**. Interestingly, we observed that DENV infection to reverse the PMA-
207 induced ERK1/2 phosphorylation at 3 days post-infection (Fig. 3B, compare lanes 3 and 4 with lane 2).
208 However, by day 6 the phosphorylation of ERK1/2 recovered significantly in infected cells when compared
209 to uninfected controls (Fig. 3B, compare lanes 6, 7 with lanes 3, 4). Nonetheless, the ratio of p-ERK/ERK
210 at 6 days post-infection was still lower in virus infected cells when compared to uninfected cells treated
211 with PMA for a similar duration (Fig. 3B, compare lanes 6 and 7 with lane 5)**.** In a manner opposite to that
212 of ERK1/2, a dephosphorylation of p38 MAPK has been similarly reported to be crucial for MK
213 development**.** We did not observe any modulation in the phosphorylation status of p38 in DENV-infected
214 cells treated with PMA for 3 or 6 days (data not shown).

215 In addition to MAPKs we compared the status of different signaling protein in the JAK-STAT pathway in
216 uninfected or DENV-infected K562 cells treated with PMA. While some effect of virus infection was
217 observed with respect to a few of these signaling mediators, most of them were unaffected. A few more
218 JAK-STAT pathway intermediaries were probed by immunoblotting but remained undetectable under
219 presently used conditions (SOCS1, PIAS1, PIAS3 and PIAS4). When compared to 0 hour the ratio of p-
220 STAT1/STAT1 showed a significant decrease upon PMA treatment at both time points (Fig. 3B, compare
221 lanes 2 and 5 with lane 1). However, although DENV replication in PMA-treated cells did not alter this
222 ratio at 3 days p.i., by 6 days p.i. the ratio showed a dramatic increase in infected cells when compared to
223 uninfected controls (Fig. 3B, compare lanes 3, 4 with 2 and lanes 6, 7 with lane 5). Further, at 6 days p.i.
224 the total STAT1 protein level was also reduced to undetectable level in infected cells (Fig. 3B, compare
225 lanes 6 and 7 with lane 5).

226 STAT3 has been suggested to promote Megakaryopoiesis and in support of this we observed an increase in
227 ratio of p-STAT3/STAT3 at 3 days after PMA treatment, which was maintained till 6 days (Fig. 3B,
228 compare lanes 2 and 5 with lane 1). However in DENV infected cells treated with PMA, the ratio of p-
229 STAT3/STAT3 at both 3 and 6 days post-treatment was significantly lower when compared to uninfected
230 controls (Fig. 3B**,** compare lane 3 with lane 2 and lanes 6,7 with lane 5). The lane 4 in this immunoblot is
231 missing due to the technical reason of sample insufficiency.

232 Although STAT2 protein level is not known to be modulated by PMA-treatment, it is known to be degraded
233 in host cells following DENV infection, in a NS5 dependent manner (Ref). We did not observe any
234 alteration in STAT2 levels with PMA-treatment of uninfected cells at either time point (Fig. 3B, compare
235 lanes 2 and 5 with lane 1). As expected however, the protein was reduced to undetectable level in DENV
236 infected cells. (Fig. 3B, compare lanes 3,4 with lane 2 and 6,7 with lane 5).

237 A downregulation of STAT5 protein has been shown to be essential for promoting development of MKs.
238 In concurrence with that, we observed a reduction in the level of this protein upon PMA-treatment starting
239 from day 0 to almost undetectable level by day 6 (Fig. 3B**,** compare lanes 2 and 5 with lane 1). No additional
240 modulatory effect was however observed by DENV infection of PMA-treated cells (Fig. 3B, compare lanes
241 3,4 with lane 2 and 6,7 with lane 5).

242 An activation of the JAK-STAT signaling upregulates inflammation, which eventually leads to expression
243 of a family of genes that suppresses this pathways and are called as Suppressor of cytokine signaling or
244 SOCS1, SOCS2 and SOCS3. In accordance with a crucial role for activated JAK-STAT pathway in Mk
245 development, expression of the SOCS3 protein has been shown to have a negative effect on
246 megakaryopoiesis. However, the SOCS3 level following PMA-treatment was observed to be unchanged at
247 either time points (Fig. 3B, compare lanes 2 and 5 with lane 1). Surprisingly, in DENV-infected cells SOCSs
248 was observed to be reduced to undetectable level by day 6 (Fig. 3B, compare lanes 6 and 7 with lane 5).

249 These results implied that DENV infection might be selectively affecting the innate antiviral and
250 inflammatory pathways in differentiating K562 cell through degradation of STAT2 and SOCS3 level and
251 interference with STAT3 phosphorylation.

252 **DENV infection inhibits polyploidy and accumulation of ROS in differentiating cells without**
253 **affecting apoptosis**

254 The biochemical changes associated with Megakaryopoiesis affect the cellular modifications. Therefore we
255 quantified the PMA-induced surface marker expression and polyploidy was compared between uninfected
256 or DENV-infected cells treated with PMA. As above, cells that were either mock-infected or infected with
257 DENV were treated with PMA-supplemented growth media soon after infection and analyzed at 3 or 6 days
258 post-treatment. The results showed a significant reduction in the surface expression of CD41/61, CD42b
259 and CD61 in DENV infected cells (Fig. 4A). Phosphorylation of the ERK1/2 MAPK has been shown to be
260 an critical modulator of polyploidy during Megakaryopoiesis. Since we observed a suppression of ERK1/2
261 phosphorylation at the early time point post-infection, a comparison of the percentage of polyploid cells at
262 both time points was quantified by PI staining. As expected the result showed a significant reduction in the
263 percentage of polyploid cells generated following DENV infection (Fig. 4B). Generation of platelet from
264 megakaryocytes has been demonstrated to be dependent on induction of apoptosis in the mother cell and
265 proceeds via a unique method of intrinsic apoptosis. In accordance with PMA-induced Megakaryopoiesis
266 in K562 cells we observed a significant increase in Annexin-V positive cells upon PMA-treatment (data
267 not shown). However, a comparison of mock-infected and DENV-infected cells treated with PMA for either
268 3 or 6 days did not show any difference in the proportion of Annexin-V positive cells (data not shown).
269 However surprisingly, a comparison of Caspase3/7 activation showed significant increase in cleavage
270 activity in virus infected cells when compared to uninfected controls at 6 days p.i. (Fig. 4C).

271 Intracellular ROS is known to be generated during megakaryopoiesis and an accumulation is
272 essential for differentiation (47). DENV replication has been shown to induce generation of reactive oxygen

273 species in infected cell (53). An estimation of the ROS accumulated in K562 cells as a result of DENV
274 infection showed slight accumulation at 6 days post-infection (Fig. 5A, compare columns 2 to 1 and 6 to
275 5). In a similar manner, when compared to levels at day 0, uninfected cells treated with PMA showed a
276 significant accumulation of ROS at both 3 and 6 days post-treatment (Fig. 5A, compare columns 3 to 1 and
277 7 to 5). We expected the ROS level in DENV infected cells that have been treated with PMA to be higher
278 than the uninfected PMA-treated controls. However, surprisingly DENV infected cells treated with PMA
279 did not exhibit additional ROS accumulation at day 3 post-treatment (Fig. 5A, compare columns 3 to 4).
280 Further, surprisingly at day 6 after PMA-treatment the ROS accumulation in DENV infected cells were
281 remarkably lower compared to uninfected PMA-treated cells (Fig. 5A, compare columns 7 to 8). This
282 suggested DENV replication in differentiating cells to impede accumulation of ROS. In corroboration we
283 observed DENV infection to have an effect similar to that of N-acetyl cysteine a biochemical known to
284 quench ROS levels (Fig. 5B**).** In conclusion, DENV infection interferes with surface marker expression in
285 addition to significantly affecting accumulation of ROS and endomitosis which are associated with
286 differentiation into megakaryocytes.

287 **PMA-induced transcriptome changes are reversed by DENV infection in differentiating cells**

288 Megakaryopoiesis is associated with profound alterations in the transcriptome of differentiating cells.
289 Similarly, innate antiviral response launched upon detection of a viral infection is also associated with
290 changes in the pattern of expression of many genes. Therefore, in order to study the interaction between
291 these two stimuli at the transcriptional level the transcriptome of mock-infected and DENV-infected cells
292 was compared after 6 days of PMA-induced differentiation. For this purpose, K562 cells either mock-
293 infected or DENV-infected were induced to differentiate using 50 nM PMA and the total RNA isolated for
294 analysis of transcriptome by next-generation sequencing. The transcriptome of both uninfected and DENV-
295 infected cells was compared to uninfected cells at 0 hour with respect to PMA-treatment. As shown in Fig.
296 6A, the transcriptome in uninfected cells underwent a profound change in more than 5000 genes showing
297 different degree of deregulation. Interestingly, the comparison between uninfected and DENV-infected

298 cells after 6 days of differentiation showed reversal in the direction of PMA-induced deregulation for a
299 number of genes (Fig. 6B.). Since our earlier result showed that DENV infection suppressed ROS
300 accumulation in differentiating cells, ROS-associated genes the PMA-induced deregulation trend of which
301 was reversed by infection were analyzed further. A heatmap of these genes showed that although alteration
302 in transcript level was moderate for most of them, a few genes were dramatically affected (Fig. 6C). This
303 included GCH1, FOXO3, GLRX5, ETHE1, CTNS, EPAS1, GFOD1 and SNCA (Fig. 6C). Among these
304 transcripts corresponding to FOXO3, CTNS and EPAS1 were higher in infected cells compared to
305 uninfected ones, whereas the others showed a relatively lower level in infected cells. FOXO3 and EPAS1
306 are transcription factors among which the former is known to be pro-apoptotic (54). Among the
307 downregulated genes the protein corresponding to GCH1, ETHE1 and SNCA are enriched platelets (55-
308 57). SNCA is also known to function in an anti-apoptotic manner although the specific role of this gene in
309 apoptosis associated with megakaryocyte differentiation is not clear yet (58).

310

311

312

313

314 **Discussions:** DENV replicates in multiple cell types and causes a range of pathological symptoms.
315 Thrombocytopenia, a prominent DENV associated pathological symptom is a consequence of both
316 impaired biogenesis and altered stability of platelets. Megakaryocytes or platelets mother cells in the bone
317 marrow are known to be permissive for DENV replication, which affects platelet biogenesis. In this article,
318 we have explored the cellular and molecular effect of DENV infection on Megakaryocyte development
319 using the phorbol ester PMA induced-differentiation model in human K562 cells. Our results show that
320 differentiation of infected K562 cells promote the replication of intracellular virus by an unknown
321 mechanism and viral replication interferes with cell signaling pathways crucial for Megakaryopoiesis,
322 particularly involving the MAPK ERK1/2 and different factors in the JAK-STAT pathway. However high
323 level of viral replication does not affect the survival of the cells. PMA-induced differentiation of K562
324 cells, as with *in vivo* Megakaryopoiesis, is associated with accumulation of intracellular ROS and our results
325 show that DENV replication suppresses the accumulation of this signaling molecule by an unknown
326 mechanism. Replication by multiple viruses is known to increase ROS in the host cell we report an unique
327 observation about DENV replication suppressing ROS accumulation under specific conditions in the host
328 cell.

329 The absolute dependence of virus life cycle on host biochemical pathways implies a profound influence of
330 host cell metabolic status on viral replication. Depending on the virus being studies, PMA a known activator
331 of protein kinase C, is known to have either positive or negative effect on virus replication (59-62). On the
332 other hand, viral infection of human monocytes can induce differentiation of these cells into Dendritic cells
333 although the implication of this is not clear yet (63). Cell cycle arrest in PMA-treated K562 cells happens
334 through upregulation of p21 and p27 in a protein kinase C (PKC)-dependent but p53-independent manner
335 (64). Inducing an arrest in the host cell cycle is quite common among human viruses with beneficial effect
336 on their replication (65). The entry of DENV is known to be influenced by the cell-cycle stage of the host
337 cell, albeit in a cell-type dependent manner (66, 67). Here we observed increased intracellular replication
338 in K562 cells that have stopped dividing in response to PMA, although the halt in cell division does not

339 lower the metabolic activity as is obvious from increase in cell size and other cellular changes. In a similar
340 manner Parvovirus B19 has been observed to infect cells of erythroblast origin with replication of the viral
341 genome being promoted by differentiation of these cells into erythroblasts (68). Although it is not clear yet
342 if the PMA-induced cell cycle stall is responsible for increasing intracellular virus replication, single-cell
343 transcriptomics study by Zanini and coworkers suggested the cell cycle status of the host cell to have no
344 effect on DENV genome replication (69). In addition to DENV, Mk cells are known to support replication
345 of other viruses like the Human Immunodeficiency Virus and Hantavirus, with the former inducing
346 apoptosis in addition to reducing the surface expression of c-Mpl (70-73). Interestingly, PMA-induced
347 differentiation of Hantavirus infected megakaryocytes augmented virus replication, as observed in this
348 study (72).

349 PMA induces rapid and profound changes in host gene expression and therefore it is possible that
350 specific promoters of viral replication are overexpressed upon PMA treatment as observed for Hepatitis C
351 virus which is benefitted by the liver cell enriched microRNA-122 (74). PMA-induced differentiation
352 correlates with increase in granularity of K562 cells, probably pertaining to platelets granules that are
353 synthesized in the megakaryocyte mother cell and transferred into platelets (75). Therefore the rate of
354 protein synthesis in these cells can be expected to be enhanced for synthesis of the proteins that will form
355 part of these granules. In face the protein content of K562 cells is significantly increased during PMA
356 induced differentiation (76).It is possible that translation of viral proteins benefits from this overall increase
357 in rate of protein synthesis. The DENV genomic RNA of DENV has a 5' end type-I cap identical to host
358 mRNAs that helps in recruiting ribosomes in addition to evading innate antiviral arsenal (77). A role for
359 enhanced host protein synthesis benefiting viral translation is corroborated from our observation that the
360 entry of DENV is not higher in differentiated cells. Another possibility is that differentiation leads to
361 suppression of specific anti-viral genes, thereby benefiting the replication.

362 Although TPO is a cytokine crucial for platelet biogenesis and mice knock-out for either the
363 cytokine or its receptor show drastically reduced levels of both mature MKs as well as circulating platelets,

364 residual level of both MKs and platelets in these mice suggest other factors to also contribute in MK
365 development and platelet formation (78, 79). Receptor interaction of TPO activates JAK2 kinase leading to
366 activation of the MAPK ERK1/2, an important regulator of cell cycle and proliferation that plays a crucial
367 role in Mk maturation (80, 81) Previous studies of Mk development using K562 cells showed PMA to
368 directly activate protein kinase C (PKC) which in turn induces ERK1/2 phosphorylation, an important
369 signaling event even for *in vivo* Megakaryopoiesis (26, 50, 82, 83). A concurrent inhibition of the MAPK
370 p38 on the other hand supports MK development, suggesting this kinase to oppose or retard ERK1/2
371 mediated changes (22). Dengue infection can activate the p38 MAPK which is responsible for enhancement
372 of pro-inflammatory cytokines and apoptosis (84, 85). We observed a reduction in the level of PMA-
373 induced ERK1/2 phosphorylation in DENV-infected cells, probably causing inhibition of endomitosis and
374 platelet-specific surface marker protein expression, although a concomitant increase in p38 phosphorylation
375 was not observed. Previous reports have conclusively shown DENV NS5 protein mediated degradation of
376 the host STAT2 infection as a major mechanism for suppression of the host innate-antiviral pathway (86).
377 We observed additional regulation of a few other members of the JAK-STAT pathway, namely STAT1,
378 STAT3 and STAT5, although it is yet clear if this is restricted to PMA-treated K562 cells or is a general
379 effect occurring in other cells too. STAT1 regulated by the transcription factor (TF) GATA-1 plays a
380 specific role in endomitosis by controlling expression of cell cycle genes like CCND1, CCND2 and
381 CCNE2TFs through the TF RUNX1 (87). PMA-induced Mk development in K562 has not been reported
382 earlier to mimic the *in vivo* differentiation with respect to regulation of STAT3 and STAT5. In a manner
383 corroborative of *in vivo* development, we observed a gradual reduction of STAT5 level in parallel with
384 progression of differentiation (24). STAT3 is phosphorylated initially on Tyr-705 which triggers
385 dimerization (88). In addition to this STAT3 can have other post-translational modifications e.g.
386 phosphorylation of S-727 or acetylation of K-685, although induction of these modifications by PMA in
387 K562 cells is not clear yet (89, 90). In our study we observed DENV infection to reverse the PMA-induced
388 STAT3 phosphorylation on Tyr-705, possibly through inhibition of the respective kinase or activation
389 specific phosphatases. In addition to phosphorylation STAT3 function can be also suppressed by Ubiquitin

390 mediated degradation or interaction with proteins that are activated downstream of the JAK-STAT pathway
391 in a negative feedback loop e.g. protein encoded by PIAS and SOCS genes (91-93). In fact SOCS3 is known
392 as a specific inhibitor of STAT3 signaling pathway, for which we expected an upregulation in infected
393 cells (90). Unexpectedly however, we observed a reduction in SOCS3 protein level by DENV infection for
394 which either mechanism or implication with respect to viral life cycle is still unclear. One of the potential
395 role for STAT3 in Megakaryopoiesis is driving accumulation of intracellular ROS levels through
396 upregulation of NOX2 expression (94). Therefore, suppression of STAT3 phosphorylation might be
397 directly affecting accumulation of ROS as observed here. Further characterization of this observation would
398 probably shed more light on the implication of this regulation.

399 Reactive oxygen species or ROS, in the form of Hydroxyl radical ($^{\cdot}OH$) or Singlet oxygen ($^{1}O_2$) or
400 Superoxide anion radical ($O_2^{\cdot -}$), are generated either in response to stimuli including metabolic
401 inflammation, exposure to pathogen or as secondary messengers in signal transduction pathway. The most
402 well characterized sources of intracellular ROS are two enzymes associated with the mitochondria namely
403 **N**icotinamide **A**denine **D**inucleotide-**Q**uinone (NADH-Q) reductase (Complex I), Q-cytochrome c
404 oxidoreductase (Complex III) and the plasma membrane associated homologs of NADPH-oxidase or NOX
405 (95-97). Intracellular ROS plays crucial role in regulation of protein tyrosine kinases and phosphatases
406 through post-translational modification (98, 99). It can also activate multiple cellular pathways including
407 MAPK, NFκB, Cell cycle genes (100). Intracellular ROS can either promote apoptosis by inducing damage
408 to the mitochondrial membrane or inhibit it through oxidation of catalytic site Cysteines on executioner
409 proteases like Caspase-3 (101). In our study suppression of ROS level coincided with activation of Caspase-
410 3 cleavage activity, although the mechanism would need further investigation to draw a direct correlation
411 between them.

412 In the BM, pluripotent hematopoietic stem cells (HSCs) reside in a relatively hypoxic area while
413 during differentiation megakaryocytes relocate to more oxygen-rich region near blood vessels from where
414 platelets can be shed into the vascular circulation (102). ROS serves a critical role in megakaryocyte

415 formation since a low level of these signaling molecules in differentiating HSCs disfavor generation of
416 (**M**egakaryocyte-**E**rythrocyte **p**rogenitors) MEP and in favor of (**G**ranulocyte-**M**onocyte **p**rogenitors) GMP
417 (103). Intracellular ROS levels are regulated through the interplay of generators (like NOXs) and mitigatory
418 pathways (like the KEAP1-NRF2 pathway) (37, 104). PMA has been shown to induce accumulation of
419 ROS in K562 cells and ROS has been shown to be responsible for polyploidy and a reduction of ROS by
420 NAC directly impacts polyploidy (43, 47). Accumulation of ROS activates the KEAP1-NRF2 pathway and
421 activation of many genes that can suppress the cellular ROS levels. ROS is produced by cellular responses
422 like Unfolded-protein response (UPR) or innate-antiviral pathway (105, 106). We observed a relatively
423 higher level of intracellular ROS with respect to uninfected cells in K562 cells that are not undergoing
424 differentiation. Since PMA-induced differentiation of K562 cells also causes ROS to accumulate in cells,
425 we expected an additive effect of DENV replication on ROS accumulation in these cells. However,
426 surprisingly DENV replication quenched intracellular ROS levels through an unknown mechanism.
427 Although evidence from previous reports would strongly indicate this suppression of ROS to be major
428 contributor to inhibition in platelet biogenesis by infection of Mk mother cells by DENV, it is still not clear
429 if the viral replication in these cells is benefited from this or not. Future studies would be directed to address
430 the exact mechanism through which DENV infection suppresses ROS accumulation in these cells and the
431 physiological relevance of this suppression for the viral life cycle.

432

433 **Acknowledgement:** The authors would like to thank Dr. Manjula Kalia, Regional Centre for
434 Biotechnology, NCR Biotech Science Cluster for careful reading of the manuscript. The Translational
435 Health Science and Technology Institute is acknowledged for providing all support for equipment and other
436 infrastructure. The Core Technology Research Initiative (CoTeRI) in the National Institute for Biomedical
437 Genomics, India is acknowledged for providing Next-generation sequencing facility. JK is supported by
438 fellowship from the University grants commission. YR is supported from fellowship in the extramural
439 research grant (BT/PR22985/MED/29/1168/2016) to SB from the Department of Biotechnology, Govt of
440 India. This work was supported by extramural research grant (EMR/2016/005796) to SB from the Science
441 and Engineering Research Board, Department of Science and Technology, Govt. of India.

442 **Materials and methods**:

443 **Cell culture, Drugs and Virus**: K562 cells were procured from the American Type Culture Collection
444 (ATCC) and cultured at 37^0C, 5% CO_2 in Iscove's modified Dulbecco's media (IMDM) supplemented with
445 Penicillin (100 U/ml), Streptomycin (0.1 mg/ml) and 10%-Fetal Bovine Serum (FBS). Vero and C6/36 cells
446 were procured from the cell line repository of the National Centre for Cell Sciences (NCCS), India and
447 cultured respectively in Minimum Essential Medium (MEM) and L15 cell culture medium supplemented
448 with 10% FBS. C6/36 cells were maintained at conditions of 28^0C and atmospheric CO_2.

449 Dengue virus serotype 2 (strain NGC) was amplified in C6/36 and the culture supernatant used as inoculum.
450 The infectious titer of the virus was determined by Focus-forming unit (FFU) assay in Vero cells. For all
451 infections, the inoculum was diluted in the respective culture media supplemented with 2% FBS, and the
452 cells were incubated with the inoculum for 2 hours at the respective culture conditions of temperature and
453 CO_2 concentration, with intermittent rocking.

454 Phorbol-12 Myristate-13 acetate (PMA, Sigma Aldrich) and N-Acetyl Cysteine were diluted in
455 recommended vehicles and stored as single use aliquots at -20^0C . Fresh dilutions of N-Acetyl-L-Cysteine
456 (Sigma) were used for every experiment.

457 **Focus-forming unit (FFU) assay**: Vero cell monolayers in 24-well plate were infected with 10-fold serial
458 dilutions of virus inoculum. The inoculum was incubated with cells for 2 hours at 37^0C and 5% CO_2 with
459 intermittent rocking. The inoculum was then discarded and complete MEM added to each followed by
460 incubation for 48 hours at 37^0C and 5% CO_2. Subsequently the cells were washed with phosphate-buffered
461 saline (PBS), fixed with 2% para-formaldehyde (PFA) and permeabilized with PBS supplemented with 0.1
462 % Triton-X-100 and 1% bovine serum albumin (BSA). The permeabilized cells were washed with PBS and
463 sequentially incubated anti-DENV primary antibody (dilution 1:400 of Mab8705, Millipore) and anti-
464 Mouse Alexa-488 conjugated secondary antibody (dilution 1:500; ThermoFisher Scientific) both diluted in
465 PBS supplemented with 1% BSA. After incubation with primary antibody, the cells were washed twice

466 with PBS before addition of secondary antibody dilutions. The fluorescent foci were visualized and
467 manually counted using a fluorescence microscope and the titer calculated as FFU/ml.

468 **Flow Cytometry Analysis**: All flow cytometry analysis were performed in a BD FACS Canto II flow
469 cytometer (BD Biosciences) under standard conditions and all raw data analyzed using Flow-Jo software.
470 For immune staining of intracellular DENV antigen, K562 cells were washed with ice-cold PBS before
471 fixation with PBS supplemented with 2% PFA and permeabilization with the same buffer containing 0.1%
472 Triton-X-100. The permeabilized cells were sequentially stained with dilution of 4G2 (purified IgG2a mAb
473 produced in the lab from Hybridoma-HB112) antibody and anti-mouse Alexa-488 conjugated secondary
474 antibody. For immune staining of surface markers, cells were washed with PBS and incubated with dilutions
475 of fluor-conjugated primary antibodies, specific to either human CD61-Phycoerythrin (PE) (BioLegend) or
476 CD41/61-(Allophycocyanin) APC (BioLegend) or human CD42b-(BD Horizon brilliant violet 421) Bv421
477 (BioLegend). Antibodies were diluted in staining buffer (PBS with 1%BSA and 0.02% Sodium Azide) and
478 cells were incubated for 1h at 4°C . Subsequently the cells were washed with PBS and analyzed by flow
479 cytometry.

480 Propidium iodide staining for polyploidy analysis: Cells were harvested by centrifugation, washed
481 twice with ice-cold phosphate-buffered saline (PBS) and fixed with 70% ethanol at 4°C for 30 min. After
482 a PBS wash cells were treated with 100µl PBS supplemented with RNase-A (200µg/ml) and incubated at
483 37°C for 30 min. Cells were then washed using PBS and the genomic DNA stained with Propidium iodide
484 (50µg/ml).

485 Annexin-V and PI staining: Apoptotic detection assays were carried out by surface labeling with the Ca2+
486 dependent phosphatidylserine-binding protein Annexin-V. Cells were harvested by centrifugation, washed
487 twice with cold PBS and then re-suspended in 1x binding buffer(Apoptosis detection Kit I # 556578, BD
488 Pharmingen) at 1x 10^6 cells/ml. A 100µl aliquot was stained by addition of 5µl FITC Annexin V and 5µl

489 PI. The reagents were mixed by gentle vortex and incubated for 15 min at RT in the dark. 400µl of 1x
490 binding buffer was added to each tube and the cells analyzed by flow cytometry within 1 hr.

491 **RNA extraction and Quantitative RT-PCR**: Total RNA from $1x10^6$ K562 cells were extracted using
492 Trizol (Takara) and purified with Qiagen RNAeasy mini kit (Qiagen), as per manufacturer's instructions.
493 Viral RNA from cell-free culture supernatant was isolated using QIAmp viral RNA mini kit (Qiagen) as
494 per manufacturer's instructions. 1.0 ug of total RNA was reverse-transcribed with ImProm-II reverse-
495 transcriptase (Promega, USA) and random hexamers (Sigma) as per manufacturer's protocol, and the cDNA
496 diluted with nuclease-free water before use for real-time PCR. Real-time PCR was performed with 2x
497 SYBR mix (Takara) in a QuantStudio-6 Flex Real-Time PCR System (Applied Biosystems) using the
498 default run program.

499 **Confocal microscopy**: K562 cells were washed with PBS, fixed and permeabilized as described earlier for
500 immunostaining purposes. The cells were stained with 2.5µl of Alexa Fluor-568 Phalloidin (Invitrogen,
501 Thermo fisher scientific) at RT for 20 min to stain for F-Actin followed by PBS wash. Cells were then
502 mounted onto glass slides using ProLong Gold Antifade Mountant supplemented with DAPI (Invitrogen,
503 Thermo fisher scientific). The fluorescence was observed and imaged in a FLUOVIEW FV3000 confocal
504 microscope (Olympus).

505 **Intracellular Caspase-3/7 activity assay**: The intracellular caspase-3/7 activity was measured using
506 Caspase-Glo 3/7 Assay (Promega). For this, 1×10^4 cells in 50 µl were mixed with an equal volume of
507 Caspase-Glo3/7 reagent in wells of 96-well luminometer plate. The plate was incubated at room
508 temperature for 3 hours and the luminescence measured using a Orion II microplate luminometer
509 (Berthold). The luminescence from culture media without cells was used as negative control.

510 **Measurement of intracellular Reactive Oxygen species (ROS)**: The intracellular ROS accumulated was
511 measure using CM-H2DCFDA probe (Life Technologies) as per manufacturer's instructions. Briefly, K562
512 cells were washed with PBS and then incubated in PBS supplemented with CM-H2DCFDA as per

513 manufacturer's instructions. The cells were then incubated at 37 °C , 5% CO_2 for 30 minutes and washed
514 twice with PBS. The fluorescence intensity was quantified in a BD FACS Canto II flow cytometer (BD
515 Biosciences) under standard conditions and the raw data analyzed using Flow-Jo software.

516 **Electrophoresis and Immunoblotting**: Cells were harvested by centrifugation at 4^0C and washed with ice
517 -cold PBS. Cells were suspended in lysis solution [250 mM NaCl, 20 mM Tris-HCl (pH 7.4), , 1% Triton
518 X-100, 1 mM EDTA, supplemented with 0.1mM PMSF and protease inhibitor cocktail] and incubated on
519 ice for 15 minutes. The lysate was clarified by centrifugation (13 000×g for 10 min at 4^0C) and the
520 supernatant collected. The total protein in the lysate was estimated using Bradford's method. 40µg of
521 whole-cell lysate was denatured, resolved in a SDS-10% gel and transferred to nitrocellulose blotting
522 membrane. The membrane was blocked with either 5% skimmed milk or 5% bovine-serum albumin (BSA)
523 and incubated with dilution of respective antibodies as per manufacturer's instructions (Cell Signaling
524 technologies). The membrane was washed, incubated with dilution of HRP-conjugated secondary antibody
525 and the bands visualized by ECL chemiluminescence.

526 **Next-generation sequencing**: The total RNA from K562 cells either uninfected or infected with DENV at
527 an MOI of 10 was extracted and purified. Total RNA from similar number of uninfected cells, harvested
528 for RNA extraction immediately after addition of PMA was used as 0 hour control. The total RNA was
529 subjected to ribosomal RNA depletion before a sequencing library was prepared for 2x100 bp end-paired
530 sequencing in Illumina HiSeq2500 platform, generating 50 million reads per sample.

531

532 **References:**

533 1. Patel SR, Hartwig JH, Italiano JE, Jr. 2005. The biogenesis of platelets from megakaryocyte
534 proplatelets. J Clin Invest 115:3348-54.
535 2. Hottz ED, Bozza FA, Bozza PT. 2018. Platelets in Immune Response to Virus and Immunopathology
536 of Viral Infections. Front Med (Lausanne) 5:121.
537 3. Martina BE, Koraka P, Osterhaus AD. 2009. Dengue virus pathogenesis: an integrated view. Clin
538 Microbiol Rev 22:564-81.
539 4. de Azeredo EL, Monteiro RQ, de-Oliveira Pinto LM. 2015. Thrombocytopenia in Dengue:
540 Interrelationship between Virus and the Imbalance between Coagulation and Fibrinolysis and
541 Inflammatory Mediators. Mediators Inflamm 2015:313842.
542 5. Fang S, Wu Y, Wu N, Zhang J, An J. 2013. Recent advances in DENV receptors.
543 ScientificWorldJournal 2013:684690.
544 6. Rodenhuis-Zybert IA, Wilschut J, Smit JM. 2010. Dengue virus life cycle: viral and host factors
545 modulating infectivity. Cell Mol Life Sci 67:2773-86.
546 7. Acosta EG, Kumar A, Bartenschlager R. 2014. Revisiting dengue virus-host cell interaction: new
547 insights into molecular and cellular virology. Adv Virus Res 88:1-109.
548 8. Simon AY, Sutherland MR, Pryzdial EL. 2015. Dengue virus binding and replication by platelets.
549 Blood 126:378-85.
550 9. Ojha A, Nandi D, Batra H, Singhal R, Annarapu GK, Bhattacharyya S, Seth T, Dar L, Medigeshi GR,
551 Vrati S, Vikram NK, Guchhait P. 2017. Platelet activation determines the severity of
552 thrombocytopenia in dengue infection. Sci Rep 7:41697.
553 10. Ojha A, Bhasym A, Mukherjee S, Annarapu GK, Bhakuni T, Akbar I, Seth T, Vikram NK, Vrati S, Basu
554 A, Bhattacharyya S, Guchhait P. 2019. Platelet factor 4 promotes rapid replication and
555 propagation of Dengue and Japanese encephalitis viruses. EBioMedicine 39:332-347.
556 11. Noisakran S, Onlamoon N, Hsiao HM, Clark KB, Villinger F, Ansari AA, Perng GC. 2012. Infection of
557 bone marrow cells by dengue virus in vivo. Exp Hematol 40:250-259 e4.
558 12. Vogt MB, Lahon A, Arya RP, Spencer Clinton JL, Rico-Hesse R. 2019. Dengue viruses infect human
559 megakaryocytes, with probable clinical consequences. PLoS Negl Trop Dis 13:e0007837.
560 13. Clark KB, Noisakran S, Onlamoon N, Hsiao HM, Roback J, Villinger F, Ansari AA, Perng GC. 2012.
561 Multiploid CD61+ cells are the pre-dominant cell lineage infected during acute dengue virus
562 infection in bone marrow. PLoS One 7:e52902.
563 14. Sridharan A, Chen Q, Tang KF, Ooi EE, Hibberd ML, Chen J. 2013. Inhibition of megakaryocyte
564 development in the bone marrow underlies dengue virus-induced thrombocytopenia in
565 humanized mice. J Virol 87:11648-58.
566 15. Basu A, Jain P, Gangodkar SV, Shetty S, Ghosh K. 2008. Dengue 2 virus inhibits in vitro
567 megakaryocytic colony formation and induces apoptosis in thrombopoietin-inducible
568 megakaryocytic differentiation from cord blood CD34+ cells. FEMS Immunol Med Microbiol 53:46-
569 51.
570 16. Akashi K, Traver D, Miyamoto T, Weissman IL. 2000. A clonogenic common myeloid progenitor
571 that gives rise to all myeloid lineages. Nature 404:193-7.
572 17. Kaushansky K. 2008. Historical review: megakaryopoiesis and thrombopoiesis. Blood 111:981-6.
573 18. Deutsch VR, Tomer A. 2006. Megakaryocyte development and platelet production. Br J Haematol
574 134:453-66.
575 19. Schulze H, Shivdasani RA. 2004. Molecular mechanisms of megakaryocyte differentiation. Semin
576 Thromb Hemost 30:389-98.

577 20. Cecchetti L, Tolley ND, Michetti N, Bury L, Weyrich AS, Gresele P. 2011. Megakaryocytes
578 differentially sort mRNAs for matrix metalloproteinases and their inhibitors into platelets: a
579 mechanism for regulating synthetic events. Blood 118:1903-11.
580 21. Matsumura I, Kanakura Y. 2002. Molecular control of megakaryopoiesis and thrombopoiesis. Int
581 J Hematol 75:473-83.
582 22. Severin S, Ghevaert C, Mazharian A. 2010. The mitogen-activated protein kinase signaling
583 pathways: role in megakaryocyte differentiation. J Thromb Haemost 8:17-26.
584 23. Kirito K, Osawa M, Morita H, Shimizu R, Yamamoto M, Oda A, Fujita H, Tanaka M, Nakajima K,
585 Miura Y, Ozawa K, Komatsu N. 2002. A functional role of Stat3 in in vivo megakaryopoiesis. Blood
586 99:3220-7.
587 24. Olthof SG, Fatrai S, Drayer AL, Tyl MR, Vellenga E, Schuringa JJ. 2008. Downregulation of signal
588 transducer and activator of transcription 5 (STAT5) in CD34+ cells promotes megakaryocytic
589 development, whereas activation of STAT5 drives erythropoiesis. Stem Cells 26:1732-42.
590 25. Beaulieu LM, Lin E, Morin KM, Tanriverdi K, Freedman JE. 2011. Regulatory effects of TLR2 on
591 megakaryocytic cell function. Blood 117:5963-74.
592 26. Racke FK, Lewandowska K, Goueli S, Goldfarb AN. 1997. Sustained activation of the extracellular
593 signal-regulated kinase/mitogen-activated protein kinase pathway is required for megakaryocytic
594 differentiation of K562 cells. J Biol Chem 272:23366-70.
595 27. Goldfarb AN. 2007. Transcriptional control of megakaryocyte development. Oncogene 26:6795-
596 802.
597 28. Tijssen MR, Ghevaert C. 2013. Transcription factors in late megakaryopoiesis and related platelet
598 disorders. J Thromb Haemost 11:593-604.
599 29. Muntean AG, Pang L, Poncz M, Dowdy SF, Blobel GA, Crispino JD. 2007. Cyclin D-Cdk4 is regulated
600 by GATA-1 and required for megakaryocyte growth and polyploidization. Blood 109:5199-207.
601 30. Lordier L, Bluteau D, Jalil A, Legrand C, Pan J, Rameau P, Jouni D, Bluteau O, Mercher T, Leon C,
602 Gachet C, Debili N, Vainchenker W, Raslova H, Chang Y. 2012. RUNX1-induced silencing of non-
603 muscle myosin heavy chain IIB contributes to megakaryocyte polyploidization. Nat Commun
604 3:717.
605 31. Lopez JJ, Palazzo A, Chaabane C, Albarran L, Polidano E, Lebozec K, Dally S, Nurden P, Enouf J,
606 Debili N, Bobe R. 2013. Crucial role for endoplasmic reticulum stress during megakaryocyte
607 maturation. Arterioscler Thromb Vasc Biol 33:2750-8.
608 32. You T, Wang Q, Zhu L. 2016. Role of autophagy in megakaryocyte differentiation and platelet
609 formation. Int J Physiol Pathophysiol Pharmacol 8:28-34.
610 33. De Botton S, Sabri S, Daugas E, Zermati Y, Guidotti JE, Hermine O, Kroemer G, Vainchenker W,
611 Debili N. 2002. Platelet formation is the consequence of caspase activation within
612 megakaryocytes. Blood 100:1310-7.
613 34. Chen S, Su Y, Wang J. 2013. ROS-mediated platelet generation: a microenvironment-dependent
614 manner for megakaryocyte proliferation, differentiation, and maturation. Cell Death Dis 4:e722.
615 35. Sardina JL, Lopez-Ruano G, Sanchez-Abarca LI, Perez-Simon JA, Gaztelumendi A, Trigueros C,
616 Llanillo M, Sanchez-Yague J, Hernandez-Hernandez A. 2010. p22phox-dependent NADPH oxidase
617 activity is required for megakaryocytic differentiation. Cell Death Differ 17:1842-54.
618 36. Mostafa SS, Miller WM, Papoutsakis ET. 2000. Oxygen tension influences the differentiation,
619 maturation and apoptosis of human megakaryocytes. Br J Haematol 111:879-89.
620 37. McCrann DJ, Eliades A, Makitalo M, Matsuno K, Ravid K. 2009. Differential expression of NADPH
621 oxidases in megakaryocytes and their role in polyploidy. Blood 114:1243-9.
622 38. Sattler M, Winkler T, Verma S, Byrne CH, Shrikhande G, Salgia R, Griffin JD. 1999. Hematopoietic
623 growth factors signal through the formation of reactive oxygen species. Blood 93:2928-35.

624 39. Eliades A, Papadantonakis N, Ravid K. 2010. New roles for cyclin E in megakaryocytic
625 polyploidization. J Biol Chem 285:18909-17.
626 40. Siddiqui NF, Shabrani NC, Kale VP, Limaye LS. 2011. Enhanced generation of megakaryocytes from
627 umbilical cord blood-derived CD34(+) cells expanded in the presence of two nutraceuticals,
628 docosahexanoic acid and arachidonic acid, as supplements to the cytokine-containing medium.
629 Cytotherapy 13:114-28.
630 41. Witt O, Sand K, Pekrun A. 2000. Butyrate-induced erythroid differentiation of human K562
631 leukemia cells involves inhibition of ERK and activation of p38 MAP kinase pathways. Blood
632 95:2391-6.
633 42. Kim KW, Kim SH, Lee EY, Kim ND, Kang HS, Kim HD, Chung BS, Kang CD. 2001. Extracellular signal-
634 regulated kinase/90-KDA ribosomal S6 kinase/nuclear factor-kappa B pathway mediates phorbol
635 12-myristate 13-acetate-induced megakaryocytic differentiation of K562 cells. J Biol Chem
636 276:13186-91.
637 43. Ojima Y, Duncan MT, Nurhayati RW, Taya M, Miller WM. 2013. Synergistic effect of hydrogen
638 peroxide on polyploidization during the megakaryocytic differentiation of K562 leukemia cells by
639 PMA. Exp Cell Res 319:2205-15.
640 44. Chaman N, Iqbal MA, Siddiqui FA, Gopinath P, Bamezai RN. 2015. ERK2-Pyruvate Kinase Axis
641 Permits Phorbol 12-Myristate 13-Acetate-induced Megakaryocyte Differentiation in K562 Cells. J
642 Biol Chem 290:23803-15.
643 45. Lee CH, Yun HJ, Kang HS, Kim HD. 1999. ERK/MAPK pathway is required for changes of cyclin D1
644 and B1 during phorbol 12-myristate 13-acetate-induced differentiation of K562 cells. IUBMB Life
645 48:585-91.
646 46. Nurhayati RW, Ojima Y, Nomura N, Taya M. 2014. Promoted megakaryocytic differentiation of
647 K562 cells through oxidative stress caused by near ultraviolet irradiation. Cell Mol Biol Lett 19:590-
648 600.
649 47. Huang R, Zhao L, Chen H, Yin RH, Li CY, Zhan YQ, Zhang JH, Ge CH, Yu M, Yang XM. 2014.
650 Megakaryocytic differentiation of K562 cells induced by PMA reduced the activity of respiratory
651 chain complex IV. PLoS One 9:e96246.
652 48. Colosetti P, Puissant A, Robert G, Luciano F, Jacquel A, Gounon P, Cassuto JP, Auberger P. 2009.
653 Autophagy is an important event for megakaryocytic differentiation of the chronic myelogenous
654 leukemia K562 cell line. Autophagy 5:1092-8.
655 49. Limb JK, Yoon S, Lee KE, Kim BH, Lee S, Bae YS, Jhon GJ, Kim J. 2009. Regulation of megakaryocytic
656 differentiation of K562 cells by FosB, a member of the Fos family of AP-1 transcription factors. Cell
657 Mol Life Sci 66:1962-73.
658 50. Rojnuckarin P, Drachman JG, Kaushansky K. 1999. Thrombopoietin-induced activation of the
659 mitogen-activated protein kinase (MAPK) pathway in normal megakaryocytes: role in
660 endomitosis. Blood 94:1273-82.
661 51. Lin YL, Liao CL, Chen LK, Yeh CT, Liu CI, Ma SH, Huang YY, Huang YL, Kao CL, King CC. 1998. Study
662 of Dengue virus infection in SCID mice engrafted with human K562 cells. J Virol 72:9729-37.
663 52. Elshuber S, Allison SL, Heinz FX, Mandl CW. 2003. Cleavage of protein prM is necessary for
664 infection of BHK-21 cells by tick-borne encephalitis virus. J Gen Virol 84:183-191.
665 53. Olagnier D, Peri S, Steel C, van Montfoort N, Chiang C, Beljanski V, Slifker M, He Z, Nichols CN, Lin
666 R, Balachandran S, Hiscott J. 2014. Cellular oxidative stress response controls the antiviral and
667 apoptotic programs in dengue virus-infected dendritic cells. PLoS Pathog 10:e1004566.
668 54. Obexer P, Hagenbuchner J, Unterkircher T, Sachsenmaier N, Seifarth C, Bock G, Porto V, Geiger K,
669 Ausserlechner M. 2009. Repression of BIRC5/survivin by FOXO3/FKHRL1 sensitizes human
670 neuroblastoma cells to DNA damage-induced apoptosis. Mol Biol Cell 20:2041-8.

671 55. Caparros-Perez E, Teruel-Montoya R, Lopez-Andreo MJ, Llanos MC, Rivera J, Palma-Barqueros V,
672 Blanco JE, Vicente V, Martinez C, Ferrer-Marin F. 2017. Comprehensive comparison of neonate
673 and adult human platelet transcriptomes. PLoS One 12:e0183042.
674 56. Majek P, Reicheltova Z, Stikarova J, Suttnar J, Sobotkova A, Dyr JE. 2010. Proteome changes in
675 platelets activated by arachidonic acid, collagen, and thrombin. Proteome Sci 8:56.
676 57. Park SM, Jung HY, Kim HO, Rhim H, Paik SR, Chung KC, Park JH, Kim J. 2002. Evidence that alpha-
677 synuclein functions as a negative regulator of Ca(++)-dependent alpha-granule release from
678 human platelets. Blood 100:2506-14.
679 58. da Costa CA, Ancolio K, Checler F. 2000. Wild-type but not Parkinson's disease-related ala-53 -->
680 Thr mutant alpha -synuclein protects neuronal cells from apoptotic stimuli. J Biol Chem
681 275:24065-9.
682 59. Polyak SJ, Rawls WE, Harnish DG. 1991. Characterization of Pichinde virus infection of cells of the
683 monocytic lineage. J Virol 65:3575-82.
684 60. Seamone ME, Wang W, Acott P, Beck PL, Tibbles LA, Muruve DA. 2010. MAP kinase activation
685 increases BK polyomavirus replication and facilitates viral propagation in vitro. J Virol Methods
686 170:21-9.
687 61. Wang W, Wang Y, Debing Y, Zhou X, Yin Y, Xu L, Herrera Carrillo E, Brandsma JH, Poot RA, Berkhout
688 B, Neyts J, Peppelenbosch MP, Pan Q. 2017. Biological or pharmacological activation of protein
689 kinase C alpha constrains hepatitis E virus replication. Antiviral Res 140:1-12.
690 62. Golding H, Manischewitz J, Vujcic L, Blumenthal R, Dimitrov DS. 1994. The phorbol ester phorbol
691 myristate acetate inhibits human immunodeficiency virus type 1 envelope-mediated fusion by
692 modulating an accessory component(s) in CD4-expressing cells. J Virol 68:1962-9.
693 63. Hou W, Gibbs JS, Lu X, Brooke CB, Roy D, Modlin RL, Bennink JR, Yewdell JW. 2012. Viral infection
694 triggers rapid differentiation of human blood monocytes into dendritic cells. Blood 119:3128-31.
695 64. Zeng YX, el-Deiry WS. 1996. Regulation of p21WAF1/CIP1 expression by p53-independent
696 pathways. Oncogene 12:1557-64.
697 65. Bagga S, Bouchard MJ. 2014. Cell cycle regulation during viral infection. Methods Mol Biol
698 1170:165-227.
699 66. Phoolcharoen W, Smith DR. 2004. Internalization of the dengue virus is cell cycle modulated in
700 HepG2, but not Vero cells. J Med Virol 74:434-41.
701 67. Helt AM, Harris E. 2005. S-phase-dependent enhancement of dengue virus 2 replication in
702 mosquito cells, but not in human cells. J Virol 79:13218-30.
703 68. Bua G, Manaresi E, Bonvicini F, Gallinella G. 2016. Parvovirus B19 Replication and Expression in
704 Differentiating Erythroid Progenitor Cells. PLoS One 11:e0148547.
705 69. Zanini F, Pu SY, Bekerman E, Einav S, Quake SR. 2018. Single-cell transcriptional dynamics of
706 flavivirus infection. Elife 7.
707 70. Zauli G, Catani L, Gibellini D, Re MC, Milani D, Borgatti P, Bassini A, La Placa M, Capitani S. 1995.
708 The CD4 receptor plays essential but distinct roles in HIV-1 infection and induction of apoptosis in
709 primary bone marrow GPIIb/IIIa+ megakaryocytes and the HEL cell line. Br J Haematol 91:290-8.
710 71. Zauli G, Catani L, Gibellini D, Re MC, Vianelli N, Colangeli V, Celeghini C, Capitani S, La Placa M.
711 1996. Impaired survival of bone marrow GPIIb/IIa+ megakaryocytic cells as an additional
712 pathogenetic mechanism of HIV-1-related thrombocytopenia. Br J Haematol 92:711-7.
713 72. Lutteke N, Raftery MJ, Lalwani P, Lee MH, Giese T, Voigt S, Bannert N, Schulze H, Kruger DH,
714 Schonrich G. 2010. Switch to high-level virus replication and HLA class I upregulation in
715 differentiating megakaryocytic cells after infection with pathogenic hantavirus. Virology 405:70-
716 80.

717 73. Zhang M, Evans S, Yuan J, Ratner L, Koka PS. 2010. HIV-1 determinants of thrombocytopenia at
718 the stage of CD34+ progenitor cell differentiation in vivo lie in the viral envelope gp120 V3 loop
719 region. Virology 401:131-6.
720 74. Henke JI, Goergen D, Zheng J, Song Y, Schuttler CG, Fehr C, Junemann C, Niepmann M. 2008.
721 microRNA-122 stimulates translation of hepatitis C virus RNA. EMBO J 27:3300-10.
722 75. Ambrosio AL, Di Pietro SM. 2019. Mechanism of platelet alpha-granule biogenesis: study of cargo
723 transport and the VPS33B-VPS16B complex in a model system. Blood Adv 3:2617-2626.
724 76. Baatout S, Chatelain B, Staquet P, Symann M, Chatelain C. 1999. Protein content and number of
725 nucleolar organizer regions are enhanced during phorbol ester-induced differentiation of cultured
726 human megakaryocytic cells. Anticancer Res 19:3229-35.
727 77. Daffis S, Szretter KJ, Schriewer J, Li J, Youn S, Errett J, Lin TY, Schneller S, Zust R, Dong H, Thiel V,
728 Sen GC, Fensterl V, Klimstra WB, Pierson TC, Buller RM, Gale M, Jr., Shi PY, Diamond MS. 2010. 2'-
729 O methylation of the viral mRNA cap evades host restriction by IFIT family members. Nature
730 468:452-6.
731 78. Gurney AL, de Sauvage FJ. 1996. Dissection of c-Mpl and thrombopoietin function: studies of
732 knockout mice and receptor signal transduction. Stem Cells 14 Suppl 1:116-23.
733 79. Kaushansky K. 2005. The molecular mechanisms that control thrombopoiesis. J Clin Invest
734 115:3339-47.
735 80. Roux PP, Blenis J. 2004. ERK and p38 MAPK-activated protein kinases: a family of protein kinases
736 with diverse biological functions. Microbiol Mol Biol Rev 68:320-44.
737 81. Fichelson S, Freyssinier JM, Picard F, Fontenay-Roupie M, Guesnu M, Cherai M, Gisselbrecht S,
738 Porteu F. 1999. Megakaryocyte growth and development factor-induced proliferation and
739 differentiation are regulated by the mitogen-activated protein kinase pathway in primitive cord
740 blood hematopoietic progenitors. Blood 94:1601-13.
741 82. Herrera R, Hubbell S, Decker S, Petruzzelli L. 1998. A role for the MEK/MAPK pathway in PMA-
742 induced cell cycle arrest: modulation of megakaryocytic differentiation of K562 cells. Exp Cell Res
743 238:407-14.
744 83. Whalen AM, Galasinski SC, Shapiro PS, Nahreini TS, Ahn NG. 1997. Megakaryocytic differentiation
745 induced by constitutive activation of mitogen-activated protein kinase kinase. Mol Cell Biol
746 17:1947-58.
747 84. Nagila A, Netsawang J, Suttitheptumrong A, Morchang A, Khunchai S, Srisawat C, Puttikhunt C,
748 Noisakran S, Yenchitsomanus PT, Limjindaporn T. 2013. Inhibition of p38MAPK and CD137
749 signaling reduce dengue virus-induced TNF-alpha secretion and apoptosis. Virol J 10:105.
750 85. Sreekanth GP, Chuncharunee A, Sirimontaporn A, Panaampon J, Noisakran S, Yenchitsomanus PT,
751 Limjindaporn T. 2016. SB203580 Modulates p38 MAPK Signaling and Dengue Virus-Induced Liver
752 Injury by Reducing MAPKAPK2, HSP27, and ATF2 Phosphorylation. PLoS One 11:e0149486.
753 86. Ashour J, Laurent-Rolle M, Shi PY, Garcia-Sastre A. 2009. NS5 of dengue virus mediates STAT2
754 binding and degradation. J Virol 83:5408-18.
755 87. Huang Z, Richmond TD, Muntean AG, Barber DL, Weiss MJ, Crispino JD. 2007. STAT1 promotes
756 megakaryopoiesis downstream of GATA-1 in mice. J Clin Invest 117:3890-9.
757 88. Yoshimura A, Naka T, Kubo M. 2007. SOCS proteins, cytokine signalling and immune regulation.
758 Nat Rev Immunol 7:454-65.
759 89. Yuan ZL, Guan YJ, Chatterjee D, Chin YE. 2005. Stat3 dimerization regulated by reversible
760 acetylation of a single lysine residue. Science 307:269-73.
761 90. Rebe C, Vegran F, Berger H, Ghiringhelli F. 2013. STAT3 activation: A key factor in tumor
762 immunoescape. JAKSTAT 2:e23010.

763 91. Wei J, Yuan Y, Jin C, Chen H, Leng L, He F, Wang J. 2012. The ubiquitin ligase TRAF6 negatively
764 regulates the JAK-STAT signaling pathway by binding to STAT3 and mediating its ubiquitination.
765 PLoS One 7:e49567.
766 92. Shuai K. 2000. Modulation of STAT signaling by STAT-interacting proteins. Oncogene 19:2638-44.
767 93. Krebs DL, Hilton DJ. 2001. SOCS proteins: negative regulators of cytokine signaling. Stem Cells
768 19:378-87.
769 94. Corzo CA, Cotter MJ, Cheng P, Cheng F, Kusmartsev S, Sotomayor E, Padhya T, McCaffrey TV,
770 McCaffrey JC, Gabrilovich DI. 2009. Mechanism regulating reactive oxygen species in tumor-
771 induced myeloid-derived suppressor cells. J Immunol 182:5693-701.
772 95. Lambeth JD. 2004. NOX enzymes and the biology of reactive oxygen. Nat Rev Immunol 4:181-9.
773 96. Zorov DB, Juhaszova M, Sollott SJ. 2014. Mitochondrial reactive oxygen species (ROS) and ROS-
774 induced ROS release. Physiol Rev 94:909-50.
775 97. Turrens JF. 2003. Mitochondrial formation of reactive oxygen species. J Physiol 552:335-44.
776 98. Salmeen A, Andersen JN, Myers MP, Meng TC, Hinks JA, Tonks NK, Barford D. 2003. Redox
777 regulation of protein tyrosine phosphatase 1B involves a sulphenyl-amide intermediate. Nature
778 423:769-73.
779 99. Lee SR, Kwon KS, Kim SR, Rhee SG. 1998. Reversible inactivation of protein-tyrosine phosphatase
780 1B in A431 cells stimulated with epidermal growth factor. J Biol Chem 273:15366-72.
781 100. Zhang J, Wang X, Vikash V, Ye Q, Wu D, Liu Y, Dong W. 2016. ROS and ROS-Mediated Cellular
782 Signaling. Oxid Med Cell Longev 2016:4350965.
783 101. Choi K, Ryu SW, Song S, Choi H, Kang SW, Choi C. 2010. Caspase-dependent generation of reactive
784 oxygen species in human astrocytoma cells contributes to resistance to TRAIL-mediated
785 apoptosis. Cell Death Differ 17:833-45.
786 102. Huang X, Trinh T, Aljoufi A, Broxmeyer HE. 2018. Hypoxia Signaling Pathway in Stem Cell
787 Regulation: Good and Evil. Curr Stem Cell Rep 4:149-157.
788 103. Shinohara A, Imai Y, Nakagawa M, Takahashi T, Ichikawa M, Kurokawa M. 2014. Intracellular
789 reactive oxygen species mark and influence the megakaryocyte-erythrocyte progenitor fate of
790 common myeloid progenitors. Stem Cells 32:548-57.
791 104. Motohashi H, Kimura M, Fujita R, Inoue A, Pan X, Takayama M, Katsuoka F, Aburatani H, Bresnick
792 EH, Yamamoto M. 2010. NF-E2 domination over Nrf2 promotes ROS accumulation and
793 megakaryocytic maturation. Blood 115:677-86.
794 105. Schwarz KB. 1996. Oxidative stress during viral infection: a review. Free Radic Biol Med 21:641-9.
795 106. Zeeshan HM, Lee GH, Kim HR, Chae HJ. 2016. Endoplasmic Reticulum Stress and Associated ROS.
796 Int J Mol Sci 17:327.

797

798

799 **Figure legends:**

800 **Figure 1: Panel A: Schematic diagram of Megakaryopoiesis**: The schematic diagram shows some of the
801 lineages that are produced during differentiation of Hematopoietic stem cells (HSC) to Megakaryocytes
802 (Mk). The formation of multilobed nucleus has also been depicted. **Panel B: Visualization of endomitosis**
803 **and multi-lobed nuclear formation following PMA-treatment.** K562 cells treated with either DMSO or
804 50 nM PMA for 6 days were stained with Alexa Fluor-568 Phalloidin, mounted onto glass slides using
805 mountant supplemented with DAPI and visualized in a confocal microscope. The red color indicates the
806 plasma membrane and blue color shows nuclei. The inset shows a cell with multilobed nucleus. **Panel C**:
807 **Expression of platelet specific surface markers:** K562 cells treated with PMA for 0, 3 or 6 days were
808 immune-stained for expression of the indicated surface marker protein using fluor-conjugated primary
809 antibodies. The mean fluorescence intensity (MFI) corresponding to each day was quantified. For each
810 surface marker the MFI at day 0 was arbitrarily set to 1 and those at day 3 and day 6, expressed as the
811 relative fold change with respect to that. The error bars represent standard deviation. The significance was
812 calculated by Student's t-test (*, **, *** respectively indicate P-values <0.5, <0.1 and <0.01). **Panel D**:
813 K562 cells treated with PMA for 0 or 3 or 6 days were fixed, permeabilized and stained for intracellular
814 DNA using Propidium iodide (PI). The PI stain was quantified by flow cytometry and mean number of
815 cells having ploidy of >4N was plotted. The error bars represent standard deviation. **Panel E:** The total
816 RNA from K562 cells treated with either DMSO or 50 nM PMA or 1mM Sodium Butyrate (NaB) for 3 or
817 6 days was extracted and purified. The total RNA was reverse transcribed using random hexamers and the
818 cDNA obtained used for real-time PCR estimation of mRNA transcripts from indicated genes. The C_T value
819 corresponding to each was normalized to that of GAPDH. The normalized value at day 0 was taken
820 arbitrarily as 1 and those at day 3 and 6 expressed as fold-change with respect to that.

821

822 **Figure 2: DENV replication is increased upon PMA treatment of infected K562 cells: Panel A:** K562
823 cells infected with DENV at an MOI of 0.1 were maintained in growth media supplemented with either
824 DMSO or 50nM PMA and fixed with PFA at 0 hour or 3 days or 6 days post-infection. The cells were
825 permeabilized and immune-stained for intracellular DENV antigen and the fluorescence quantified by flow
826 cytometry. The fluorescence in cells fixed at 0 hour was used to gate for DENV antigen positive cells. The
827 number of antigen positive cells were quantified and plotted. The error bars represent standard deviation
828 and the significance was calculated by Student's t-test (*** indicates P <0.001). **Panel B**: Total RNA from
829 K562 cells treated similarly as in panel A was extracted, purified and reverse-transcribed using random
830 hexamers. The cDNA was used for real-time PCR comparison of DENV RNA level at 3 or 6 days to that
831 at 0 hour, normalized to that of GAPDH mRNA. The value at 0 hour was taken arbitrarily as 1 and that at
832 other time points expressed as fold-change over that. The error bars represent standard deviation and the
833 significance was calculated by Student's t-test (** indicates P <0.01). **Panel C**: The culture supernatant of
834 cell infected with MOI of 0.1 and subsequently treated as in panel A was collected and used for
835 quantification of focus-forming unit/ml (FFU/ml) on Vero cell monolayers. The FFU/ml for each sample
836 was transformed to their logarithmic value to the base of 10 and plotted. The error bars represent standard
837 deviation and the significance was calculated by Student's t-test (** indicates P <0.01). **Panel D**:
838 Uninfected K562 cells treated with either DMSO or PMA for 3 days were washed with PBS and incubated
839 in either mock- or DENV inoculum (10 MOI) on ice for 2 hours. The cells were then transferred to 37^0C
840 and further incubated for 2 hours. Subsequently cells were washed, treated with 0.25% trypsin for 5 minutes
841 and the total RNA extracted and purified. 1.0 μg of total RNA was reverse-transcribed with random
842 hexamers and the cDNA used in real-time PCR for comparison of DENV genomic RNA normalized to
843 GAPDH transcripts. The level in mock-infected cells was taken as 1 and that in DENV infected cells
844 calculated as fold-change over that. The relative enrichment of DENV RNA compared to mock-infected
845 cells was quantified, transformed to their logarithmic value to the base of 2 and plotted. The error bars show
846 standard deviation and the statistical significance was calculated by Student's t-test (ns= not significant).

847

848 **Figure 3: DENV replication in differentiating K562 cells interfere with PMA-induced signaling:**
849 **Panel A:** Schematic showing comparison of signaling activated upon TPO binding to c-Mpl and by PMA.
850 **Panel B: Immunoblot for signaling protein activated by PMA in K562 cells**. K562 cells either mock-
851 infected or DENV-infected were incubated in PMA-supplemented growth media and the total protein
852 extracted after 3 or 6 days. The protein in each lysate was denatured, resolved in SDS-PAGE and
853 immunoblotted for proteins indicated at right. Immunoblot for b-actin was performed for each batch of
854 lysate used. The relative molecular mass of the marker protein is indicated on the left. **Panel C:**
855 **Quantification of immunoblot bands in panel B**. the intensity of the immunoblot band for indicated
856 proteins were quantified, normalized to that of b-actin and the ratio calculated before plotting. The error
857 bars represent standard deviation of the ratio derived from at least two independent experiments, performed
858 in multiple replicates.

859 **Figure 4: Effect of DENV replication on cell surface marker, polyploidy and apoptosis in**
860 **differentiating K562 cells. Panel A: Suppression of platelet-specific surface marker protein**. K562
861 infected with DENV at two different MOI, were incubated in PMA-supplemented growth media for 3 or 6
862 days. Subsequently the cells were immune-stained for the indicated surface marker proteins and the
863 fluorescence quantified by flow cytometry. The mean fluorescence intensity was plotted. The error bars
864 show standard deviation derived from at least two independent experiments in multiple replicates. **Panel**
865 **B: DENV replication inhibits endomitosis**. DENV infected K562 were incubated in PMA-supplemented
866 growth media for 3 or 6 days. Subsequently the cells were fixed and stained with propidium iodide and the
867 fluorescence intensity measured by flow cytometry. The number of cells with ploidy of >4N were quantified
868 and plotted. The error bars show standard deviation of the mean from two independent experiments
869 performed in multiple replicates. **Panel C: Caspase cleavage assay in differentiated DENV infected**
870 **cells**. Mock-infected or DENV-infected K562 were incubated in either DMSO or PMA-supplemented
871 growth media for 3 or 6 days. Subsequently the cells were incubated with an substrate that can be cleaved

872 by intracellular Caspase3/7 to generate a luminescent product. The luminescence was measured in a
873 luminometer and plotted. The total luminescence at day 3 in DMSO-treated uninfected cells was arbitrarily
874 taken as 1 and the rest plotted as fold-change over that. The error bars show standard deviation of the mean
875 from two independent experiments performed in multiple replicates.

876 **Figure 5: DENV infection suppresses ROS generated during PMA-induced Megakaryopoiesis in**
877 **K562 cells: Panel A**. Mock-infected or DENV-infected K562 cells were incubated in either DMSO or
878 PMA-supplemented growth media for 3 or 6 days. Subsequently the cells were stained with H_2DCFDA and
879 the fluorescence quantified by flow cytometry. The mean fluorescence intensity in mock-infected and
880 DMSO-treated cells at 3 days was arbitrarily taken as 1 and the rest calculated as fold-change over that.
881 The error bars show standard deviation of the mean from two independent experiments performed in
882 multiple replicates. **Panel B**. K562 cells either mock-infected or DENV-infected were immediately
883 incubated in growth media supplemented with 50 nM PMA in addition to either 0 or 1 or 3 mM N-Acetyl
884 Cysteine (NAC) as indicated. At 3 or 6 days post-infection the cells were stained with H_2DCFDA and the
885 fluorescence quantified by flow-cytometry. The mean fluorescence intensity in mock-infected cells treated
886 with PMA and 0 mM NAC was arbitrarily taken as 1 and that in the rest expressed as fold change with
887 respect to that. The error bars show standard deviation of the mean from two independent experiments
888 performed in multiple replicates.

889 **Figure 5: DENV replication interferes with PMA-induced transcriptome changes. Panel A**: The
890 transcriptome in K562 cells treated with 50 nM PMA for 6 days was compared to that after 0 hour by Next-
891 generation sequencing. The genes differentially expressed after 6 days of treatment, either upregulated by
892 ≥ 1.5 fold or downregulated by ≤ 0.5 fold with a P-value of ≤ 0.05, when compared to 0 hour were used to
893 draw a Volcano plot prepared using in-house written Python script. The X-axis represents the logarithmic
894 value to the base of 2 of the fold-change in gene expression. The Y-axis represents the negative logarithmic
895 to the base of 10 of the P-value. **Panel B**: The transcriptome in K562 cells, either uninfected or DENV-
896 infected and treated with 50 nM PMA or 6 days was compared to uninfected cells at 0 hour by NGS to find

897 differentially expressed genes. The level of differential expression of each gene was then compared between
898 uninfected and DENV-infected cells to draw the list of genes the PMA-induced deregulation of which is
899 influenced by infection. A volcano plot was prepared from this list using in-house written Python script.
900 The X-axis represents the logarithmic value to the base of 2 of the fold-change in gene expression. The Y-
901 axis represents the negative logarithmic to the base of 10 of the P-value. **Panel C**: **Heatmap of genes**
902 **associated with ROS-pathway**. The genes that are associated with the ROS-pathway in panel B were
903 selected and enriched using the Metascape software. The PMA-induced fold-change in the transcript level
904 of these genes after 6 days when compared to uninfected cells treated with PMA for 0 hour (column 1) in
905 either uninfected cells (column 2) or DENV-infected cells (column 3), was represented by a heatmap
906 prepared using the Morpheus algorithm (https://software.broadinstitute.org/morpheus). The colors
907 represent the trend of deregulation corresponding to each gene shown on the right.

908

Figure 1

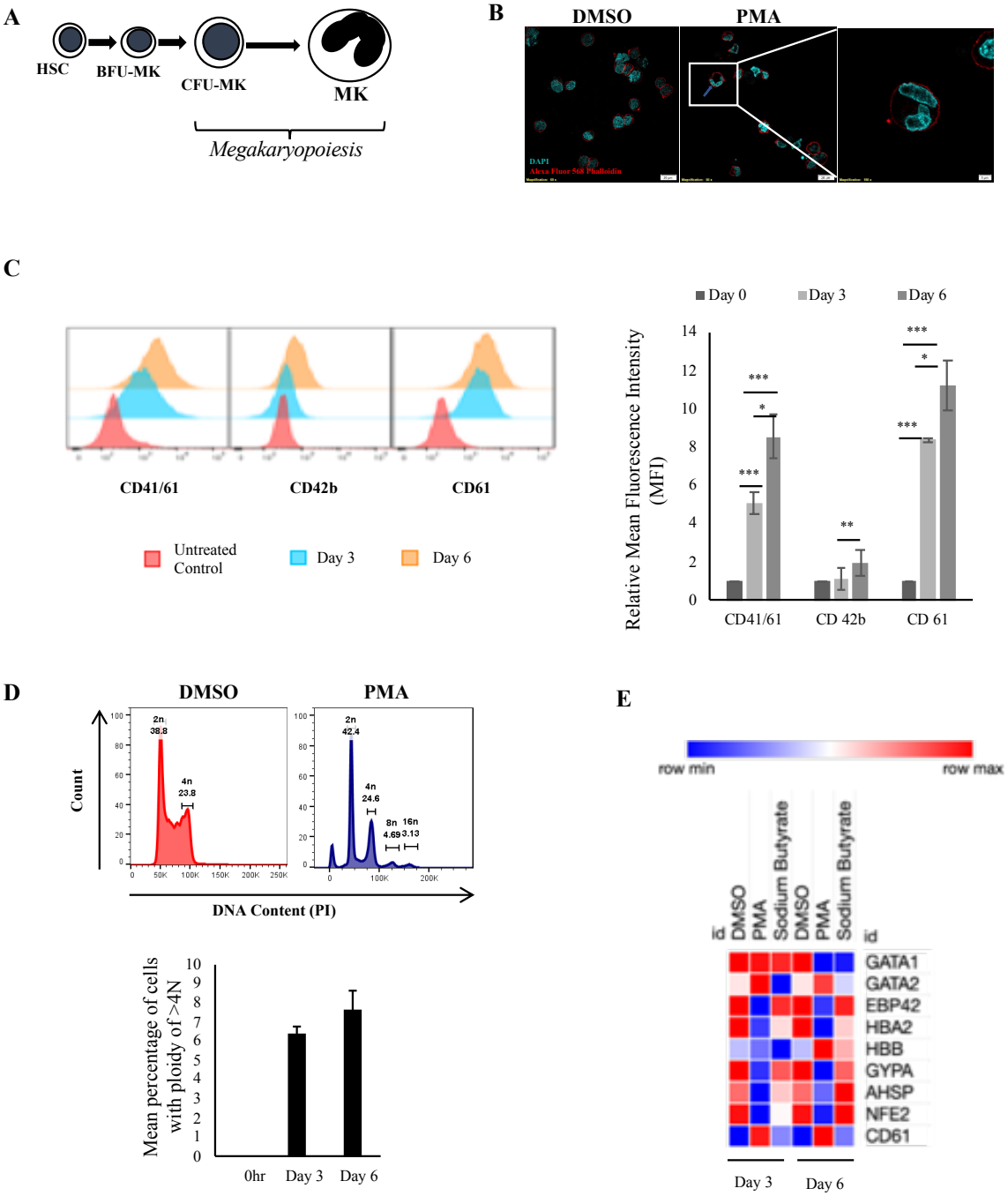
A
HSC
BFU-MK
CFU-MK
MK
Megakaryopoiesis
B
DMSO
PMA
DAPI
Alexa Fluor 568 Phalloidin
C
CD41/61
CD42b
CD61
Untreated Control
Day 3
Day 6
Day 0
Day 3
Day 6
Relative Mean Fluorescence Intensity (MFI)
CD41/61
CD 42b
CD 61
D
DMSO
PMA
Count
2n 38.8
4n 23.8
2n 42.4
4n 24.6
8n 4.69
16n 3.13
DNA Content (PI)
Mean percentage of cells with ploidy of >4N
0hr
Day 3
Day 6
E
row min
row max
id
DMSO
PMA
Sodium Butyrate
DMSO
PMA
Sodium Butyrate
id
GATA1
GATA2
EBP42
HBA2
HBB
GYPA
AHSP
NFE2
CD61
Day 3
Day 6

912

Figure 2

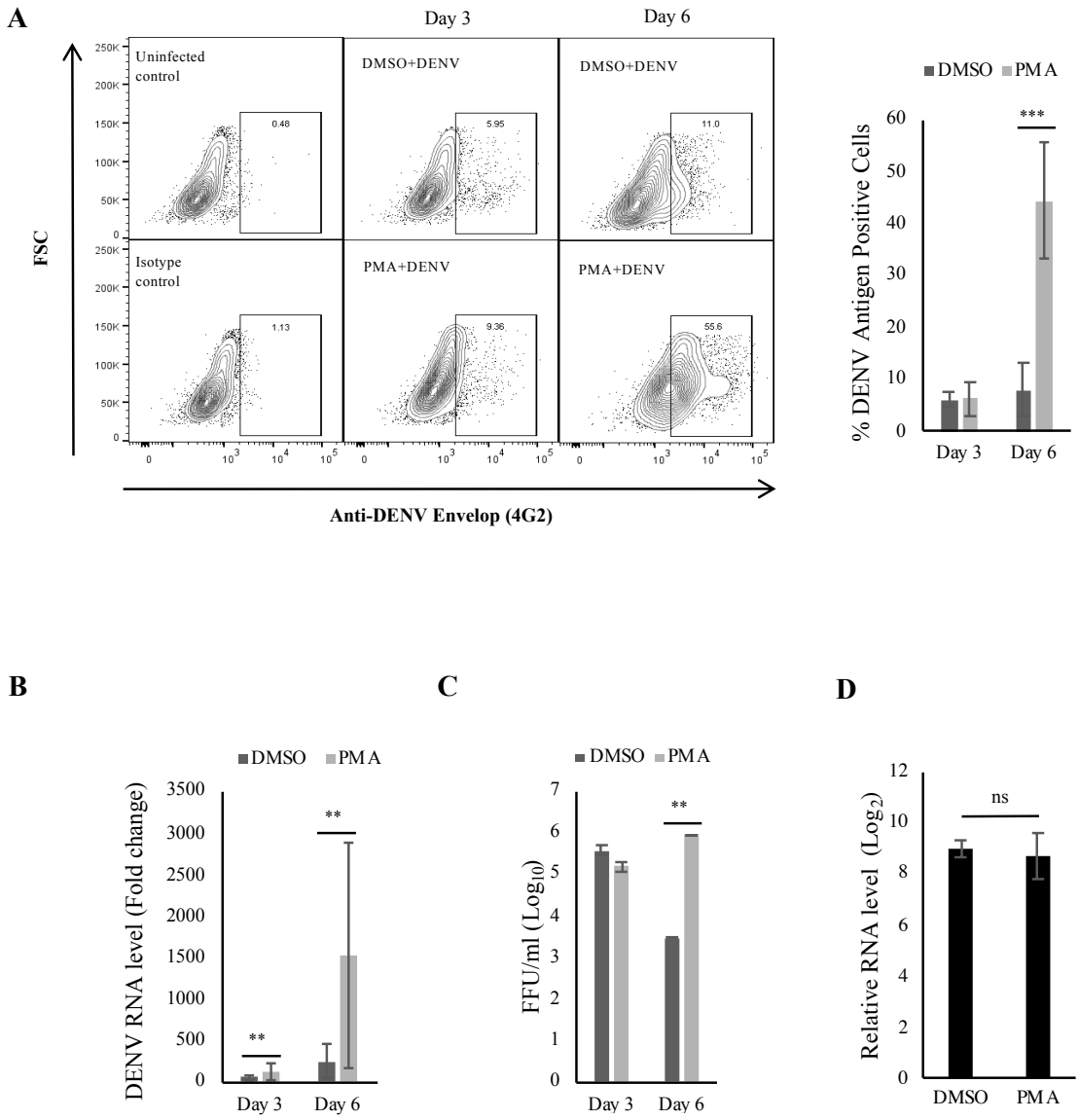

913

914

Figure 3

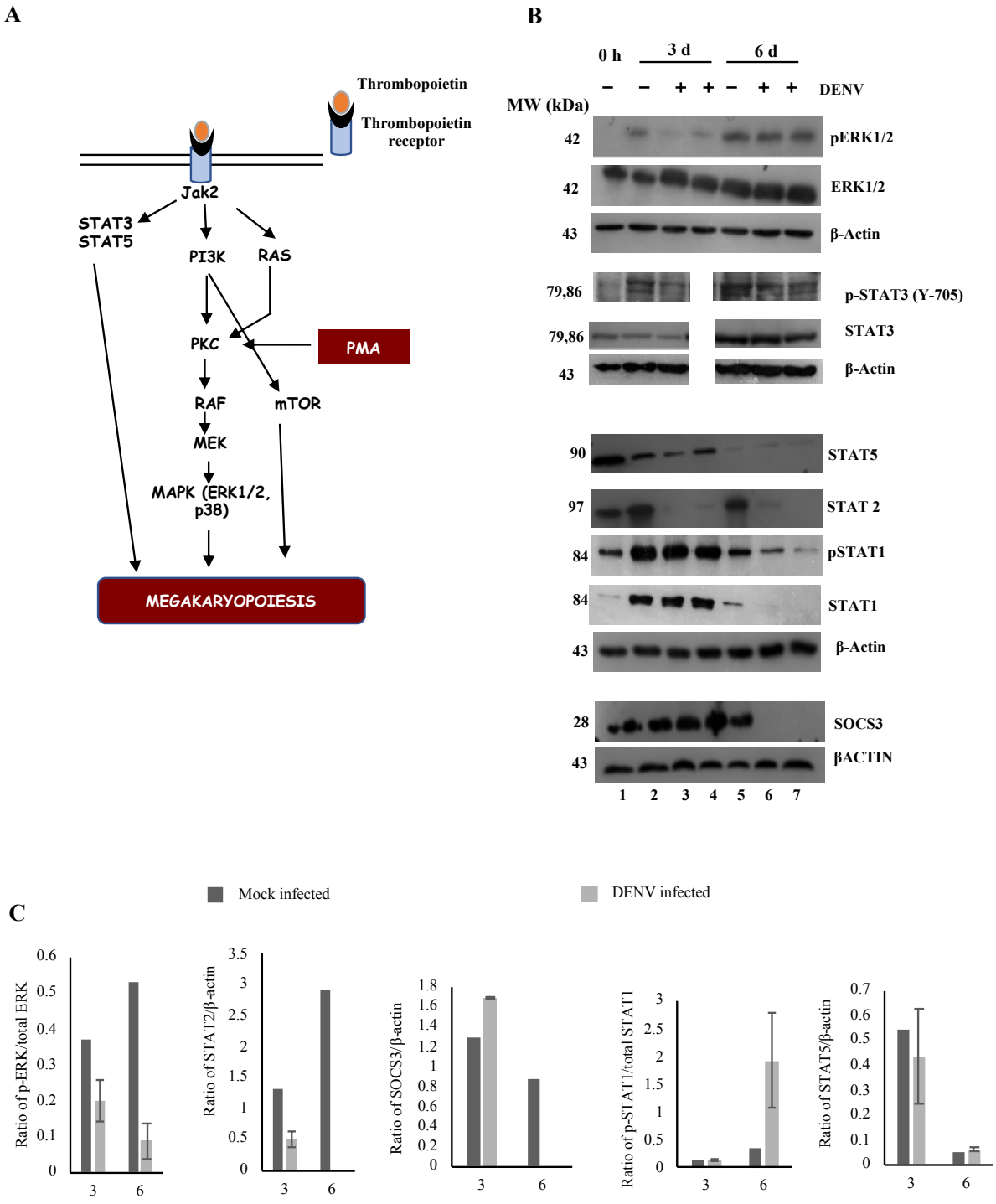

915

Figure 4

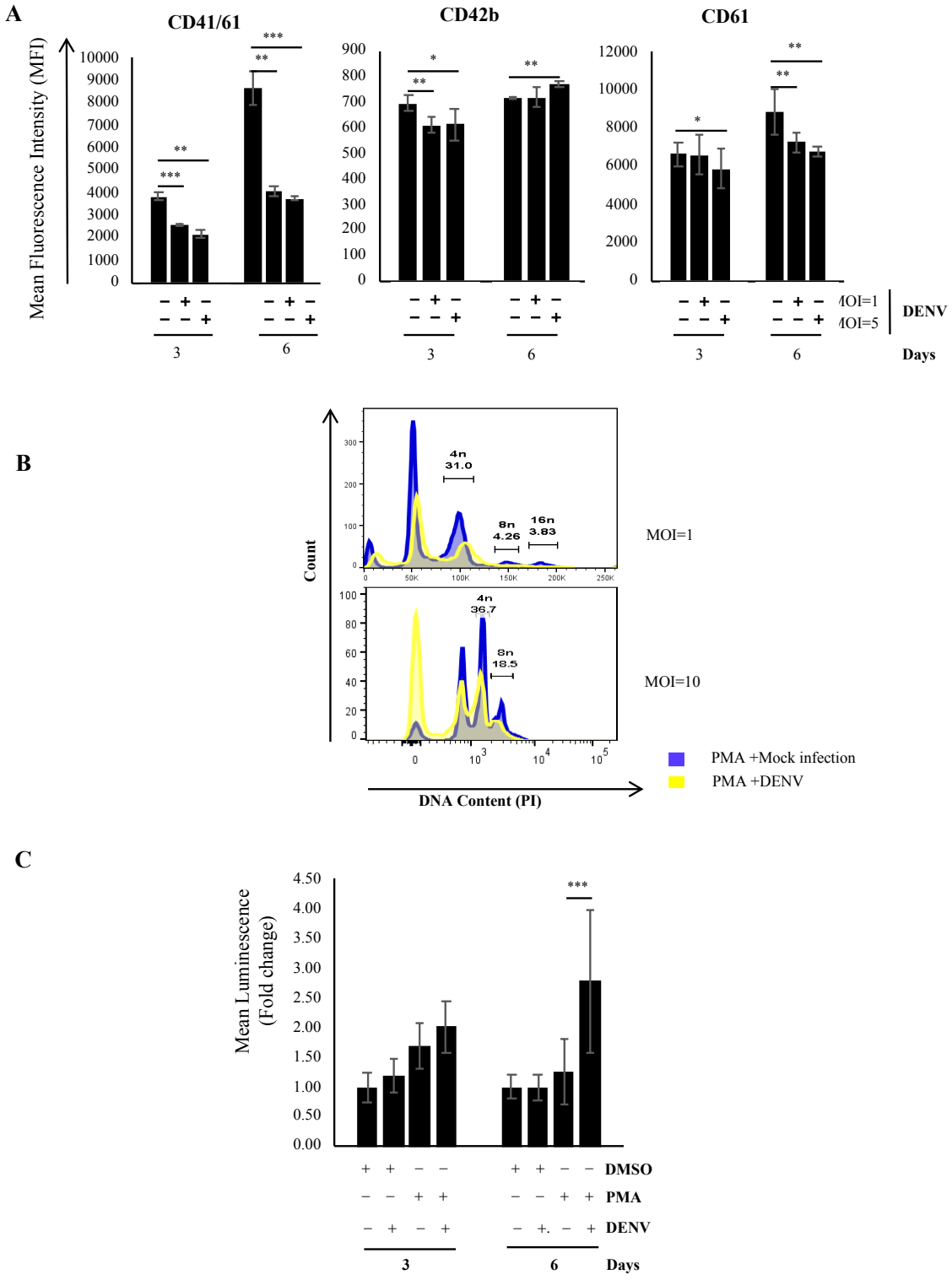
A
CD41/61
CD42b
CD61
Mean Fluorescence Intensity (MFI)
MOI=1
MOI=5
DENV
Days
B
Count
4n 31.0
8n 4.26
16n 3.83
MOI=1
4n 36.7
8n 18.5
MOI=10
PMA +Mock infection
PMA +DENV
DNA Content (PI)
C
Mean Luminescence (Fold change)
DMSO
PMA
DENV
Days

Figure 5

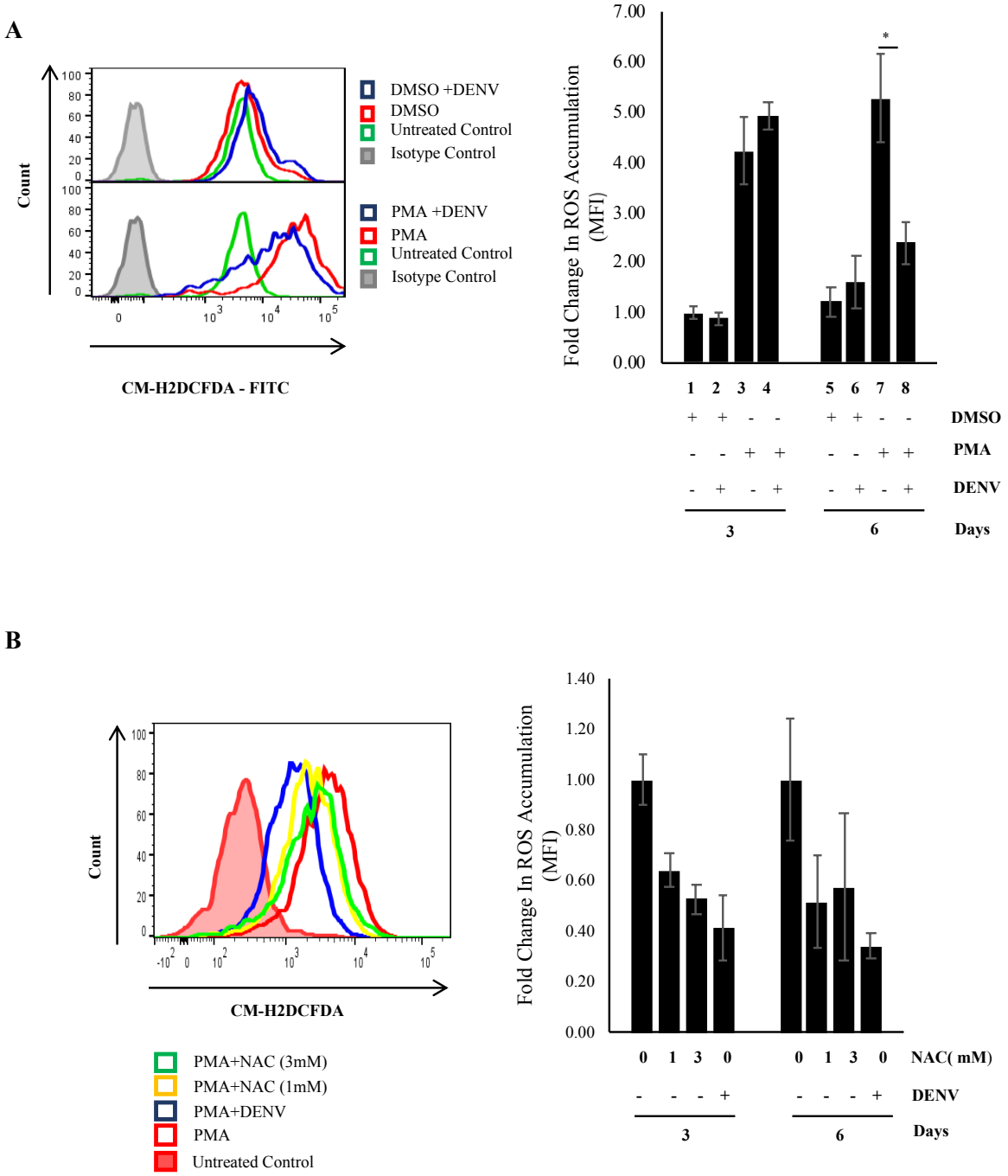
A
Count
CM-H2DCFDA - FITC
DMSO +DENV
DMSO
Untreated Control
Isotype Control
PMA +DENV
PMA
Untreated Control
Isotype Control
Fold Change In ROS Accumulation (MFI)
DMSO
PMA
DENV
Days
B
Count
CM-H2DCFDA
PMA+NAC (3mM)
PMA+NAC (1mM)
PMA+DENV
PMA
Untreated Control
Fold Change In ROS Accumulation (MFI)
NAC(mM)
DENV
Days

Figure 6

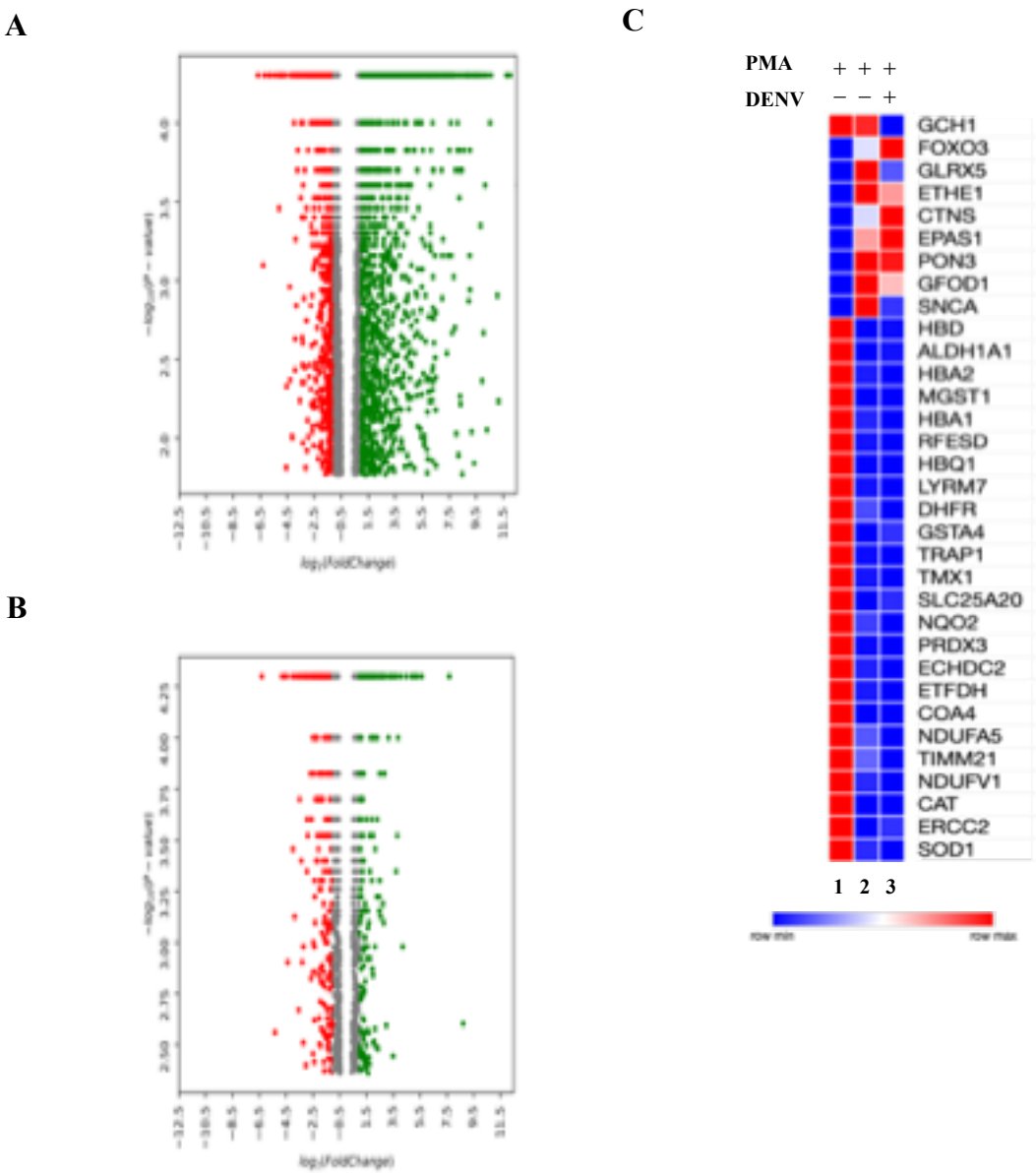
A
B
C
PMA + + +
DENV − − +
GCH1
FOXO3
GLRX5
ETHE1
CTNS
EPAS1
PON3
GFOD1
SNCA
HBD
ALDH1A1
HBA2
MGST1
HBA1
RFESD
HBQ1
LYRM7
DHFR
GSTA4
TRAP1
TMX1
SLC25A20
NQO2
PRDX3
ECHDC2
ETFDH
COA4
NDUFA5
TIMM21
NDUFV1
CAT
ERCC2
SOD1
1 2 3

920